

PEOPLE'S DEMOCRATIC REPUBLIC OF ALGERIA
MINISTRY OF HIGHER EDUCATION AND SCIENTIFIC RESEARCH
KASDI- MERBAH OUARGLA UNIVERSITY
FACULTY OF HYDROCARBONS, RENEWABLE ENERGIES, EARTH AND
THE UNIVERSE SCIENCE
RENEWABLEENERGIES DEPARTMENT



Dissertation

Presented to obtain a diploma of
ACADEMIC MASTER DEGREE

Specialty: Renewable energies

Presented by:

LEZGHEM MOHAMED YUCEF

Theme:

Optimization and Simulation of H-Darrieus Vertical
Wind Turbine using ANSYS® 18.2

Publicly supported on: 11/06/2018

Board of the jury:

- | | | |
|-------------------------|--------------------------|-----------|
| ➤ Mr. Bouchekima Bachir | University of KM Ouargla | President |
| ➤ Mr. Dernouni Amhamed | University of KM Ouargla | Examiner |
| ➤ Mr. Douak Mohamed | University of KM Ouargla | Reporter |

Academic year : 2017/2018

ACKNOWLEDGEMENTS

I would like to express my gratitude to my mentor Mr. DOUAK MOHAMED for his invaluable guidance. Without his advice this thesis would not have been possible.

I also would like to gratefully acknowledge my hearty appreciation to my advisory committee: PR. BOUCHEKIMA BACHIR and Mr.DERNOUNI AMHAMED.

I am forever indebted to my mother for her endless patience, encouragement and love when it was most required. I owe a debt of gratitude to my wife and my daughter Manissa, to my family, to my classmate ,for there countless support.

I am also thankful to all those people who are directly or indirectly associated with me and whose contribution made this project attain a successful completion.

Thank you all.

Lezghem Mohamed Youcef

Table of Contents		Page
Acknowledgement		I
Table of contents		II
Figure list		III
Table list		IV
Nomenclature and Abbreviation		V
General Introduction		1
Chapter I: Wind Turbine Overview		
I.1	Introduction	3
I.2	Theoretical Background	3
I.2.1	Betz's law	4
I.2.2	Tip Speed Ratio	5
I.2.3	Power Curve	6
I.2.4	Forces Involved	7
I.2.5	Turbulence	8
I.3	Types of Wind Turbines	8
I.3.1	Horizontal Axis Wind Turbines	8
I.3.1.1	Principle	9
I.3.1.2	Advantages	10
I.3.1.3	Disadvantages	10
I.3.2	Vertical Axis Wind Turbines	10
I.3.2.1	Savonius Rotor	13
I.3.2.2	Darrieus Rotor	14
I.3.2.3	H-Darrieus Rotor	16
I.3.3	Characterization of Vertical Axes Wind Turbines (VAWT's)	17
I.3.3.1	Two blades Vs. Three Blades	17
I.4	Algeria wind speed Potential	18
I.5	Conclusion	18
Chapter II: Wind Turbine Overview		
II.1	Introduction	19
II.2	Equations Governing	19
II.3	Assumptions	19
II.3.1	Continuity Equation	20
II.3.3	Equation of momentum following x	20
II.3.3	Equation of momentum following Y	20
II.4	The turbulence model	20
II.4.1	ModelK- ϵ	20
II.4.1.1	Modeled equation of ϵ	22
II.4.1.2	Models of constants	22
II.4.1.3	Mach Number	22
II.4.2	SST k-omega turbulence model	23
II.4.3	Turbulence Intensity	24
II.5	Number of Reynolds	25
II.6	Conclusion	25
Chapter III: Wind Turbine Overview		
III.1	Introduction	26
III.2	Designing and Optimization of VAWT	26

III.2.1	Choose the turbine size	27
III.2.2	Choose the optimized Tip Speed Ratio (TSR)	28
III.2.3	Calculate the optimal angle of Attack	28
III.2.4	Choose the best AIRFOIL	29
III.3	Simulation and Setup using ANSYS 18.2	31
III.3.1	ANSYS Overview	31
III.3.2	ANSYS WorkFlow	32
III.3.2.1	Creating Geometry using Design Modular	32
III.3.2.1.1	1st Step: Creating a Project file in ANSYS Workbench	34
III.3.2.1.2	2nd Step: Creating the Geometry	35
III.3.2.2	Creating Mesh (3rd Step)	38
III.3.2.2.1	Fixed Domain (Edge Sizing 1)	38
III.3.2.2.2	Fixed Domain (Edge Sizing 2)	39
III.3.2.2.3	Fixed Domain: Face Meshing	39
III.3.2.2.4	Meshing Rotating Domain:	41
a-	Meshing the Airfoils	41
b-	Meshing the Interface	42
c-	Mesh Quality Check (Skewness Factor)	44
d-	Name the Boundary Conditions	45
III.3.2.3	Solver Setup (4 th Step)	46
III.3.2.3.1	General and Module	46
III.3.2.3.2	Materials	47
III.3.2.3.3	Cell Zone Conditions	47
III.3.2.3.4	Boundary Conditions	48
III.3.2.3.5	Mesh Interface	50
III.3.2.3.6	Reference Values	50
III.3.2.4	Solution Setup (5 th Step)	51
III.3.2.4.1	Methods	51
III.3.2.4.3	Controls	52
III.3.2.4.3	Monitor	53
III.3.2.4.4	Initialization	53
III.3.2.4.5	Run Calculation	54
III.4	Conclusion	54
CHAPTER IV: Results and discussion		
IV.1	Introduction	55
IV.2	Pressure Contour	55
IV.3	Velocity Contour	56
IV.4	Turbulence Kinetic Energy Contour	57
IV.5	Velocity Vector	58
VI.6	Pressure Vector	59
IV.7	Validating the coefficient of Performance	
IV.8	Conclusion	60
Conclusion and Recommendations		61-62
Reference		
Appendix		
Abstract		

Figures List

Figure I- 1 Type of wind turbines.....	4
Figure I- 2 Power Coefficient plot.....	5
Figure I- 3: Power Coefficient curve for different types of turbines.....	6
Figure I- 4: Power curve.....	7
Figure I- 5: The effect of lift and drag forces.....	9
Figure I- 6: Types of VAWT's.....	12
Figure I- 7: Working principal of a Savonius rotor.....	13
Figure I- 8: Three blades Savonius turbine.....	14
Figure I- 9: Working principal of Darrieus rotor.....	15
Figure I- 10: Darrieus "eggbeater" turbine.....	15
Figure I- 11: H-Darrieus rotor.....	16
Figure I- 12: Annual maps of wind speed in Algeria at 10 m high.....	18
Figure III- 1: Design optimization work flow.....	26
Figure III- 2 The optimized turbine size on 3D.....	27
Figure III- 3: Cl/Cd ratio for various Angle of Attack.....	29
Figure III- 4: Proposed Airfoil profiles.....	30
Figure III- 5: lift to drag ratio for different airfoil profile.....	30
Figure III- 6:NACA0018 profile and characteristics.....	30
Figure III- 7: ANSYS Workbench windows overview.....	31
Figure III- 8: ANSYS Workflow description.....	32
Figure III- 9: Geometrical dimension of the field study.....	33
Figure III- 10: Schema of Rotating Domain.....	34
Figure III- 11:Creating a Project Flow in ANSYS Workbench.....	34
Figure III- 12: Importing Airfoil Data into SpaceClaim.....	35
Figure III- 13: Creating NACA0018 profile with the Angle of Attack.....	35
Figure III- 14: Move the blade by R=1 m.....	36
Figure III- 15: Creating a 3 Airfoil using a Circular Pattern.....	36
Figure III- 16: Create a Rotating Domain.....	37
Figure III- 17: Creating a Fixed Domain.....	37
Figure III- 18: Mesh Quality check.....	38
Figure III- 19: Edge Sizing 1.....	38
Figure III- 20: Edge sizing 2.....	39
Figure III- 21: Face Meshing.....	39
Figure III- 22: Fixed Domain Mesh Generation.....	40
Figure III- 23: Meshing the Airfoils.....	41
Figure III- 24: Meshing the Interface.....	42
Figure III- 25: Rotating Domain Mesh Generation.....	43

Figure III- 26: Mesh Around the Airfoils	43
Figure III- 27: Rotating and Fixed Domain Mesh Generation.....	44
Figure III- 28: Skewness values for the generated Mesh.....	44
Figure III- 29: Fixed Domain Boundary Conditions	45
Figure III- 30: Rotating Domain Boundary Conditions.....	45
Figure III- 31: Fluent Launcher Setup	46
Figure III- 32: General and viscous Model setup	46
Figure III- 33: Material Editor Panel	47
Figure III- 34: Cell Zone Conditions Setup	47
Figure III- 35: Inlet Setup	48
Figure III- 36: Outlet Setup.....	49
Figure III- 37: Airfoils and Walls Setup.....	49
Figure III- 38: Mesh Interface Setup.....	50
Figure III- 39: Reference Values Setup	50
Figure III- 40: Solution Methods Setup	51
Figure III- 41: Solution Controls Setup	52
Figure III- 42: Residual Monitors Setup.....	53
Figure III- 43: Initialization Setup	53
Figure III- 44: Run Calculation and check setup	54
Figure IV- 1: Static Pressure Contour simulation results	55
Figure IV- 2: Velocity Contour simulation results	56
Figure IV- 3: Turbulence kinetic energy Contour simulation results	57
Figure IV- 4: Velocity vector Distribution	58
Figure IV- 5: Velocity streamline	58
Figure IV- 6:Pressure vector Distribution.....	59
Figure IV- 7: Reported Moment Coefficient by FLUENT	60

Table list

Table I- 1: Comparison of VAWT's and HAWT's	12
Table II- 2: Coefficients of standard K- ϵ Model.....	22
Table II- 1: Equation terms definition.....	23
Table III- 1 Ouargla Wind Speed.....	27
Table III- 2: Main geometrical features of the analysed rotor	33
Table III- 3: Fixed Domain Mesh Data Summary	40
Table III- 4: Rotating Domain Mesh Data Summary	42
Table III- 5: Velocity Inlet input summary	48
Table III- 6: Pressure Outlet input summary	48
Table III- 7: Solution Methods input summary	51
Table III- 8: Solution Controls input summary.....	52

Nomenclature

P	Wind power	(W)
P_{tc}	The turbine power coefficient	
$T P$	Wind turbine power	(W)
M	Momentum	(Nm)
ω	Radial velocity	(m/s)
ρ	Density	(kg/m ³)
S	Surface	(m ²)
L	Reference length	(m)
mc	Momentum coefficient	
$TSR(\lambda)$	Tip speed ratio	
D	Wind Turbine Diameter	(m)
R	Wind turbine radius	(m)
N	Number of round	(RPM)
C	Blade's chord	(m)
σ	Solidity	
H	Wind turbine height	(m)
SST	Shear stress transport	
k	Turbulence kinetic energy	
ε	Dissipation coefficient	
ω	Specific dissipation rate	
Y	Non-dimensional wall distance	
Y	The distance to the nearest wall	
$w \tau$	The wall shear stress	
ν	The local kinematics viscosity	
Re	Reynolds Nombre	
u	Speed at x Axe	(m/s)
C_{μ}	Dimensionless coefficient	
V	Wind Speed	(m/s)
\vec{v}	Wind speed vector(m/s)	
V_{∞}	Wind speed not perturbe	(m/s)
W	Relative Wind speed	(m/s)
y	Distance to wall	(m/s)
α	AttackAngle	(deg)
μ	Dynamic viscosity	(N-s/m ²)
T_{mean}	Torque	(N-m)

ABBREVIATIONS

AR Aspect Ratio

CFD Computational Fluid Dynamics

DNS Direct Numerical Simulation

LES Large Eddy Simulation

NSE Navier Stokes Equation

RANS Reynolds Averaged Navier Stokes

RNG Renormalization Group

S-A SpalartAllmaras

S k- ϵ Standard k- ϵ

SST K- Ω Shear Stress Transport K- Ω

General Introduction

Vertical Axis Wind Turbines (VAWTs) are becoming ever more important in wind power generation thanks to its compactness and adaptability for domestic installations. However, it is well known that VAWTs have lower efficiency, above all if compared to HAWTs. To improve VAWTs performance, industries and researchers are trying to optimize the design of the rotors. Some numerical codes like Vortex Method or Multiple Streamtube Model have been developed to predict VAWTs performance and optimize efficiency but these codes are based on 1D simplified equation and they need accurate experimental data for aerodynamic coefficients of the airfoils. Furthermore they do not provide information on the wakes and they use semi empirical equations to predict effects like tip vortex and dynamic stall. These codes are so mainly used to do a first attempt design and the results have to be validated using wind tunnel experiments. However, as the wind tunnel experiments are expensive in terms of both costs and time, another way to study aerodynamic behavior of the rotors is to use CFD.

As it is known, CFD resolves the fluid dynamic equations and it is certainly more realistic than the 1D models but there are many other problematic issues like stall and turbulence modeling, unsteady rotational effects and long computation time. Some works were found in scientific literature regarding the application of CFD modeling on VAWTs.

In this study the authors will present the strategy of generating a 2D CFD model to predict H-Darrieus rotors performance and solve such issues.

Particularly, the CFD model was developed using ANSYS Workbench 18.2 multi-physics platform. The study was based on the conclusion of previous researches and study performed in this scope of work.

In this project consist of designing the optimum vertical wind turbine for an average wind speed of 3.8 m/s for Ouargla region, furthermore, a 3 blades rotor with NACA 0018 symmetrical airfoil was chosen as one of the best airfoil comparing to different profile presented in Chapter III, First step was to generate a simplified CAD and optimize the computational domain. Then a sliding mesh was generated to best understand the phenomena and confirm the results, refining the mesh till the results obtained with different grids were applied. The turbulent model was a challenging parameter that best approaches the reality, therefore, both a realizable K- ϵ with an Enhanced wall treatment and K- ω was selected to best simulate the turbulence around the rotating domain.

General Introduction

As the unsteady rotational effects are very important in VAWTs, an unsteady Sliding Mesh Model with non-conformal mesh was used. Time step of the transient model was optimized also.

Simulations were performed on a DELL LATITUDE E6410, with 2 Intel Quad Core Xeon M560 processors (2.67 GHz) and 8 GB of RAM memory installed. A parallel computing technique was implemented in ANSYS Fluent solver.

The objective of this project is to optimize the design of VAWT in Ouargla region by running a 2D CFD simulation by using ANSYS 18.2 software after defining the optimum rotor dimension, Therefore, The project will be splinted into four main chapters as per below:

1. Chapter I: Overview about the various wind turbines and more precisely about the H-Darrieus wind turbine.
2. Chapter II: Mathematical Methodology where the governing equations used by the software Fluent.
3. Chapter III: Designing and optimizing our H-Darrieus VAWT workflow and the steps to setup the ANSYS workbench from the beginning till the solver and results.
4. Chapter IV: Simulation results and Discussion.

The use of the Transition model leads to a good prediction of trend of mechanical power and power coefficient with an overestimation of 6-8 % due to the well-known limits of the 2D models, However, in order to best optimize the proposed H-Darrieus wind turbine a 3D simulation is required with an efficient machine.

Chapter I
Wind Turbine Overview

Chapter 01

Wind Turbine Overview

I.1 Introduction

Before we reproduce the design and run the simulations, we will first explore wind energy technologies and focus more on vertical turbines and more specifically H-Darrieus vertical wind turbines which called also **Vertical Axes Wind Turbine (VAWT)**.

I.2 Theoretical Background

Wind is an inexhaustible energy source available all around the world. In fact, on shore energy is extremely large and reported to be from $20,000 \cdot 10^9$ kWh to $50,000 \cdot 10^9$ kWh [1]. In 2014, the International Energy Agency (IEA) reported that the global electricity generation reached $23903 \cdot 10^9$ kWh . The potential onshore wind energy is of course not entirely usable, as the wind might be too slow or too fast for practical applications. Some of the locations are also very remote and very far from consumption hubs, making the energy transportation not economically viable.

Wind turbine sizes vary drastically and have known massive developments in the last decades. The average size in the 1980s was less than 100 kW ; nowadays the size can reach up to 8 MW like the Vestas V164, a horizontal axis offshore wind turbine .

There are two types of Wind turbines: the widely spread and most deployed Horizontal Axis Wind Turbine (HAWT), and the less popular Vertical Axis Wind Turbine (VAWT) as shown in Figure I-1. We will explore these types in details in the coming sections.

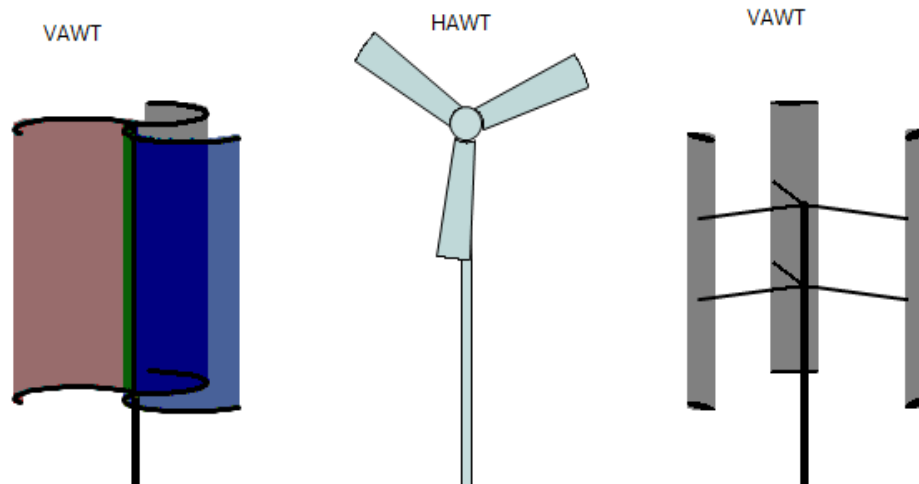


Figure I- 1Type of wind turbines

The principle behind wind turbines is simple, and humanity has been making good use of it for centuries. The kinetic energy from the flow of a mass of air is transformed to rotational kinetic energy. This rotational energy is then used as mechanical energy to run machine parts to pump water out of a well, mill grains, or generate electricity[1].

I.2.1 Betz's law

Betz law, named after German physicist Albert Betz, states the maximum theoretical efficiency that any wind turbine can attain. It states that there is a maximum power that can be extracted from a flow of air. Because of conservation of momentum and of mass, energy can never be fully extracted from wind. Betz proved that the maximum kinetic energy that can be extracted from the wind cannot exceed $16/27$ (59.3%). Thus according to this law, no turbine can extract all the speed out of the flowing wind, and the wind will always have a flow after passing through the turbine.

Figure I-2 is a plot that shows the power coefficient of a turbine C_p (the ratio of the extracted power to the available power) vs. the ratio of the speed of the wind before and after passing through the turbine:

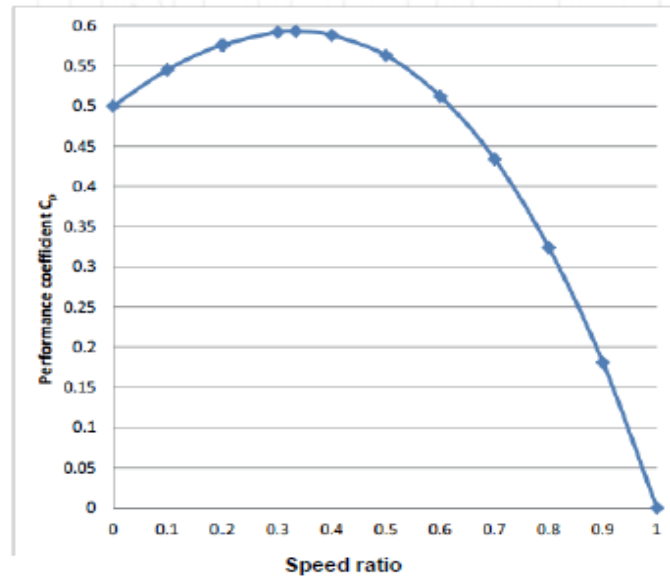


Figure I- 2Power Coefficient plot

The derivation of the Betz limit is based on a horizontal axis wind turbine, and does not apply directly to vertical turbines. The same source argues even that this theoretical limit can be exceeded using an ideal VAWT system. However, it is reported that VAWTs are less efficient than HAWTs, and are less likely -in their current state- to exceed the limit for horizontal axis turbine[1].

I.2.2 Tip Speed Ratio

The tip speed ratio (λ) is the ratio of the speed of the tip of the blades to the speed of the wind

$$\lambda = \frac{v_{tip}}{v_{wind}} \quad (\text{I-1})$$

As the tip speed ratio varies, so does the power coefficient and hence the efficiency of the turbine. An optimal value that will result in the maximum C_p is desired. Figure I-3 shows the C_p lambda curve for different types of wind turbines as cited in:

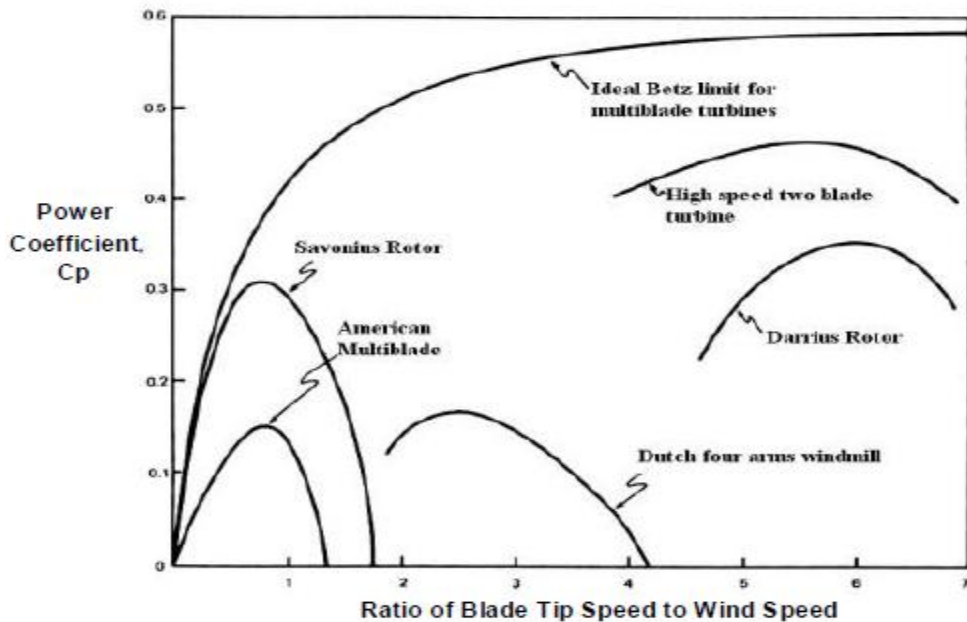


Figure I- 3: Power Coefficient curve for different types of turbines

Low tip speed ratio means not enough energy is extracted from the wind, and consequently a low C_p . A high wind tip ratio can also result in low C_p , as well as high stresses in the blades. Therefore, it is very important to have the optimal tip speed ratio, to maximize the efficiency[1].

I.2.3 Power Curve

The power curve is a plot that describes the performance of a wind turbine at different wind speeds. It shows the electrical energy power output vs. the wind speed, and gives an idea about the minimum and maximum wind speeds for a wind turbine.

Figure I-4 shows a typical power curve as obtained from:

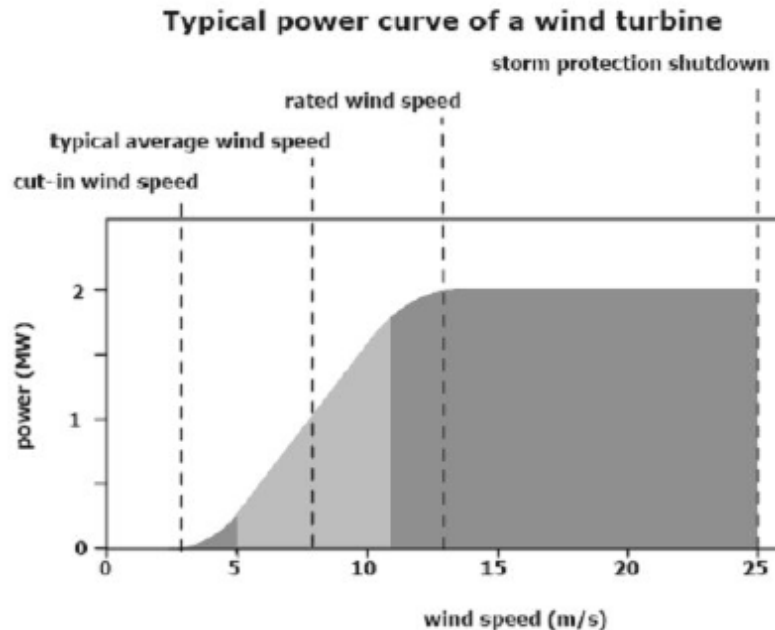


Figure I- 4: Power curve

The power generated is of course less than the extracted kinetic energy, as it has to go through a gearbox, and a generator, and both have efficiencies less than 100%.

Every turbine has its own minimum necessary wind speed to run, as shown in the Figure. Turbines are usually shut down at high speeds to prevent mechanical failure that would lead to a catastrophic failure of the turbine system[1].

I.2.4 Forces Involved

There are two types of forces that cause the wind turbines to rotate. These are drag and lift. Drag force has the same direction as the fluid flow (wind in our case), and lift forces are perpendicular to the direction of the flow. Depending on the type of the blades used, a turbine could be using either lift or drag to cause the rotational motion. Horizontal turbines as we will see in the following sections, utilize the lift force on their blades whereas Savonius turbines make use of the drag force to push the blades[2].

I.2.5 Turbulence

Turbulence is defined as “instability or disturbance” as well as unpredictability of the weather (wind speeds, direction, duration ...).

Turbulence presents a major challenge for wind turbines as it makes the generation profile inconsistent and decreases the lifetime of turbine blades because of the mechanical stresses. Accordingly, predicting turbulence is as important as predicting the general weather conditions. The random and sudden changes in wind speed and direction pose many challenges on the turbine components. These components have to be able to accommodate short duration of peak loads at times of high turbulence, and have to be mechanically strong to resist the vibrations generated from the turbulent flow.

There are other concepts and variables that impact the performance and characteristics of turbines, such as twist angle of the blades of HAWTs, pitch angle, friction ..., however as our project deals with H-Darrieus wind turbine we only discuss the concepts that are most pertinent to this specific type of turbines. We will review other factors in details in the section detailing H-Darrieus VAWTs[2].

I.3 Types of Wind Turbines

I.3.1 Horizontal Axis Wind Turbines

As mentioned before horizontal axis wind turbines are the most mature and widely used wind turbines on the planet. In this section, we will briefly look at the principal, advantages, and challenges of this type of turbines. There are multiple factors that determine design of horizontal wind turbine, from material choice for the blades and stress distribution, to turbulence effects and vibrations. As this project deals principally with H-Darrieus vertical wind turbines, we will only give a brief introduction of HAWTs[1].

I.3.1.1 Principle

Any turbine whose rotor is connected to a horizontal shaft is a horizontal axis wind turbine. The rotor's blades rely on lift in order to make the turbine rotate. This is a result of the aerofoil shape of the blades of the HAWTs.

The airfoil blade design works like an airplane wing. The difference of pressure between the two sides of the blade results in a lift force that is perpendicular to the blade and hence makes it rotate. Figure I-5 shows the effect of lift and drag [1]:

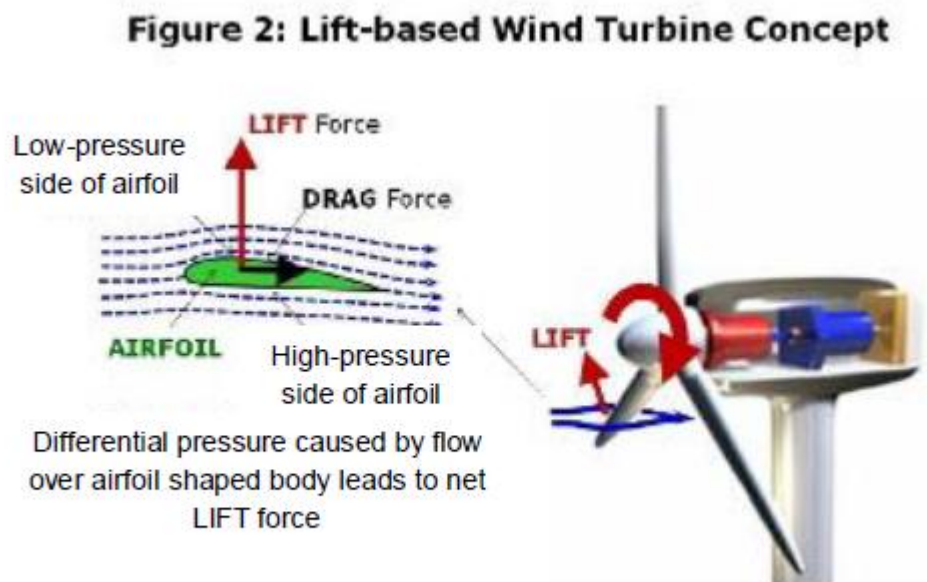


Figure I- 5:The effect of lift and drag forces

They usually have two or three blades, and the diameter and the height vary depending on the power output needed. The higher the tower, the higher the wind speed, and the longer the blades, the larger the area swept and the power output. The rotor is attached to a shaft which goes through a gearbox and then to a generator. A good blade design suitable for a wind turbine is one with a high lift to drag ratio, as this maximizes the power output of the turbine. By designing the

blade in such a way to maximize lift and minimize drag, most of the wind energy is going to turn the rotor, and hence produce more power [1].

I.3.1.2 Advantages

As all renewable energy sources, HAWTs are a clean and sustainable energy source, with a great potential. HAWTs particularly have a “high generating capacity, improved efficiency, variable pitch blade capability, and tall tower base structure to capture large amounts of wind energy”. Their massive sizes, allows for large-scale generation, and their variable pitch angle allows for using an optimal angle of attack which increases their efficiency. HAWTs are based on a very mature technology, and their high efficiencies offer a very competitive energy source for both onshore and offshore applications. However, they do have many disadvantages discussed in the following section.

I.3.1.3 Disadvantages

One of the most negative aspects of HAWTs is that they are extremely noisy. This usually makes them less socially acceptable than other renewable sources. HAWTs are very difficult to design and build. There are many variables that go into designing the perfect blade for a horizontal wind turbine, this makes them rather expensive and difficult to maintain. They require a strong support to carry the heavy load and resist vibrations. HAWTs also require an expensive and sophisticated yaw mechanism to turn the rotor, as they always have to face the direction of the wind[2].

I.3.2 Vertical Axis Wind Turbines

The main reason behind developing Vertical Axis Wind turbines is that they work regardless of the wind direction. VAWTs do not require a yaw mechanism and are very fixed in the sense that no change to their direction or that of the blade is made once installed. The lack of a yaw mechanism is one of the reasons VAWTs are not as expensive or complicated to make. This makes them ideal for small-scale applications such as remote areas with very small electric load. Their blades do not require a mechanism to change their angle as they work with any wind direction. VAWTs are considerably less noisy than HAWTs, which makes them more socially accepted. In addition to this, the small size means they can be integrated easily within an urban setting, and present no danger to the wildlife in rural areas.

They still share many components with HAWTs however, such as the shaft, the gearbox, the tower, and the generator unit. The placement of these units is different, since in VAWTs the gearbox and generator are placed at the base of the unit and do not require as much support as HAWTs. This means easier access for maintenance and repairs, which lowers the overall cost of such systems.

As mentioned before, the way the Betz limit is derived uses some assumptions that are not applicable to VAWTs. However, in general VAWTs are far less efficient than HAWTs.

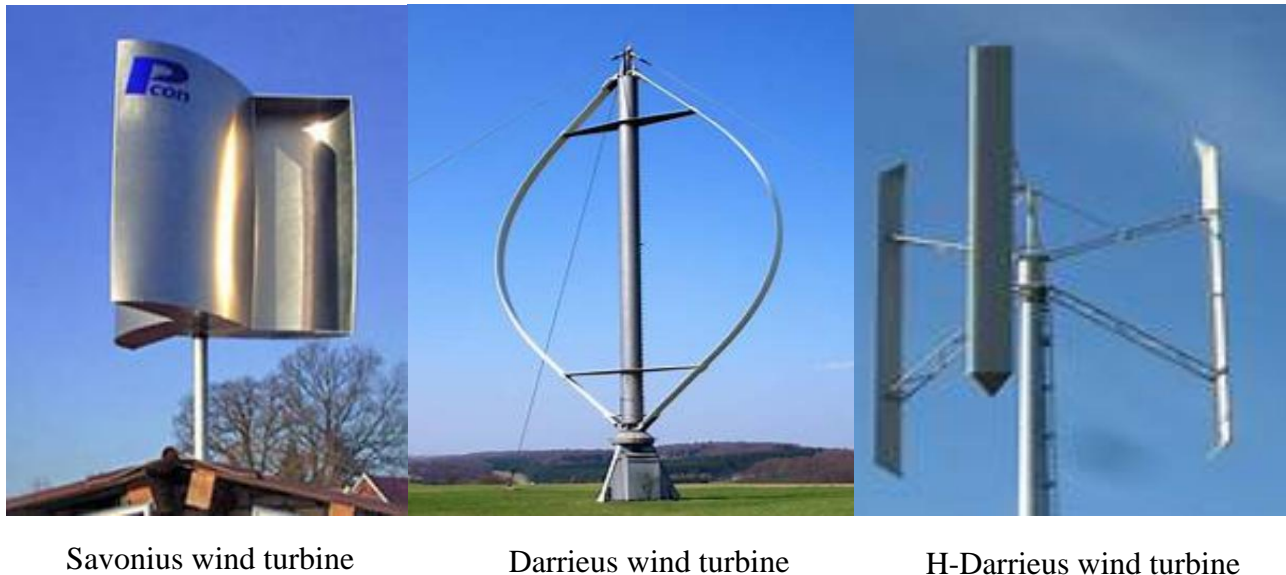
Their small capacity makes them ideal for light load application such as communication systems in remote areas. VAWTs can be used for large capacity installations, but the materials needed and the massive investment make them undesirable. VAWTs are also suitable for either low wind speeds at which HAWTs do not function or high wind speeds at which HAWTs are shut off. As stated in, “a HAWT can achieve higher efficiencies, but only if the energy quality of the wind is high. High wind turbulence, wind fluctuations, and high directional variability can cause significant problems for a HAWT, whereas VAWTs can operate well”[5].

Table I-1 below is a summary comparison of the characteristics and performance of VAWTs and HAWTs :

Table I- 1: Comparison of VAWT's and HAWT's

	VAWTs	HAWTs
Tower Sway	Small	Large
Tower Mechanism	No	Yes
Overall Formation	Simple	Complex
General Location	On ground	Not on ground
Height from Ground	Small	Large
Blade's operation space	Small	Large
Noise produced	Low	Relatively high
Wind direction	Independent	Dependent
Obstruction for Birds	Low	High

As shown in Figure I-6, there exist three types of rotors for the Vertical Axis Wind Turbines: the Darrieus rotor, the H-Darrieus rotor, and the Savonius rotor .



Savonius wind turbine

Darrieus wind turbine

H-Darrieus wind turbine

Figure I- 6:Types of VAWT's

I.3.2.1 Savonius Rotor

Savonius wind turbine was invented by the Finnish engineer Sigurd Savonius in 1922. Its most basic design is S-shaped with two blades.

The Savonius turbine uses drag to push the curved blades to generate a torque that will make the rotor turn. Aerodynamically it is the simplest wind turbine to design and build which reduces its cost drastically compared to the aerofoil blade designs of the other VAWTs and HAWTs.

Its working principle is extremely simple. The turbine rotates because of the difference of the drag force acting on the concave and convex parts of its blades. Figure I-7 illustrates this principle:

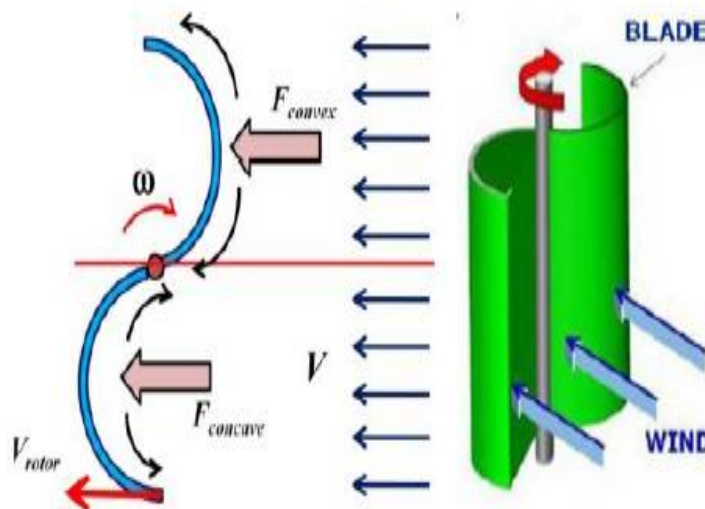


Figure I- 7: Working principal of a Savonius rotor

The air is trapped in the concave part and pushes the turbine. The flow that hits the convex part does produce a drag that is lower than the one on the concave part. It is the differential of the drag force that causes this turbine to rotate.

This lowers the efficiency of the turbine as some of the wind's power is used in pushing the convex part and is hence "wasted". More blades can be added to the S shape design, and the same principle causes it to spin as shown in Figure I-8:

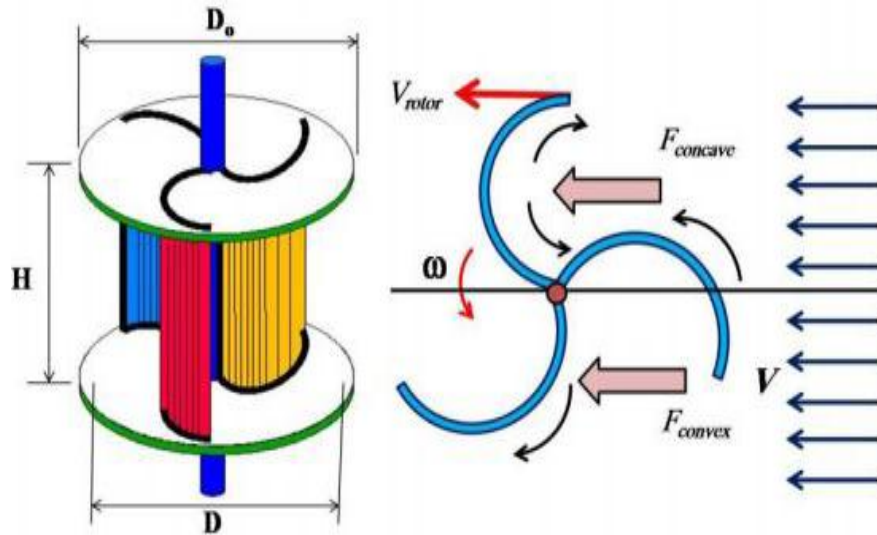


Figure I- 8:Three blades Savonius turbine

A Savonius rotor requires 30 times more surface for the same power as a conventional rotor blade wind-turbine. Therefore it is only useful and economical for small power requirements.” This makes Savonius ideal for small applications with low wind speeds. Savonius are hence desirable for their reliability, as they are able to work at several magnitudes of wind speed[1].

I.3.2.2 Darrieus Rotor

Darrieus turbines are vertical turbines whose blades are aerofoils that use lift force to turn the rotor and generate electricity. They were designed and first fabricated by the French aeronautical engineer Georges Jean Marie Darrieus in the 1920s. Their working principle is quite different from that of horizontal axis turbines, even though they both rely on the forces of lift. After the turbine starts rotating, the motion of its blades through the air creates an apparent wind that is relative to the rotating blades. This relative airflow is added to the wind resulting in a force combination. This creates a force that causes a net positive torque in the rotor, making it rotate in the same direction it had originally. If the Darrieus turbine is stationary, most of the time the wind will not cause it to move, as it is the combination of the airflow resulting from the motion of the blades and the wind that sustains the motion, and not just the wind. The Darrieus rotor has

to be started by spinning it until it reaches its operation speed, which represents a major disadvantage. Figure I-9 illustrates its working principle.

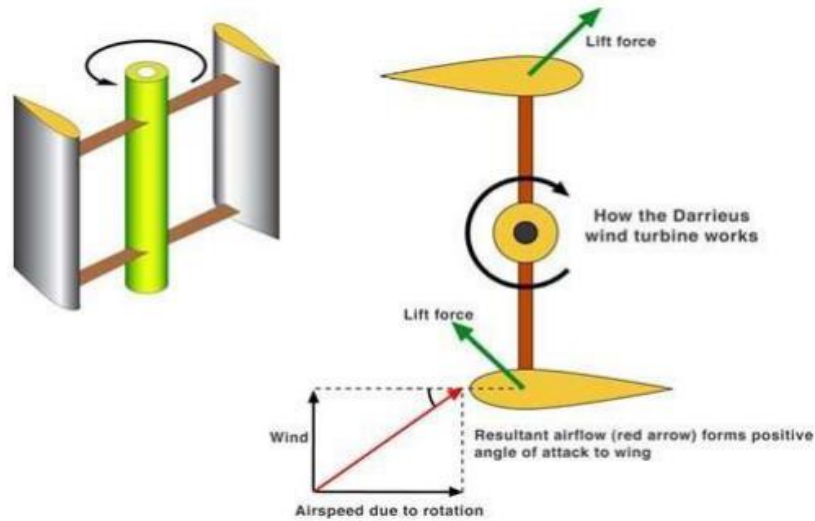


Figure I- 9:Working principal of Darrieus rotor

The Darrieus rotor takes the shape of an eggbeater. This curved shape minimizes the bending moments that result from the centrifugal forces that are exerted on the rotating blade.

Figure I-10 shows an example of a Darrieus eggbeater turbine



Figure I- 10:Darrieus "eggbeater" turbine

The shape of the blades in these designs is quite difficult and expensive to manufacture (airfoil, curvature). This led to the development of a second type of Darrieus turbines discussed in the next section[1].

I.3.2.3 H-Darrieus Rotor

The H-Darrieus rotor, also known as the Giromill rotor, is a more efficient version of the Darrieus rotor. Its blades are easier to manufacture and offer greater efficiency, making it more attractive both technically and economically. Straight blades replace the curved blades and use the same principal to operate. The two blades version of the Giromill forms the shape of the letter H, and hence the name. Its blades can either be fixed or have a variable pitch depending on the needs, and some of the variable pitch designs are able to self-start.

Figure I-11 shows the most common 3 blades H-Darrieus rotor VAWT:



Figure I- 11:H-Darrieus rotor

There are other less common experimental variations of the Darrieus rotor, but the ones discussed are the most used and researched. The last type we will discuss is the Savonius Wind Turbine, the focus of this project [2].

I.3.3 Characterization of Vertical Axes Wind Turbines (VAWT's)

Every vertical wind turbine is characterized by the swept area A_s . This area influences the energy output of the turbine, and the larger it is, the more energy the turbine collects. $A_s = H * D$ where H is the height of the turbine and D is its diameter.

The tip speed ratio of the rotor is defined by the equation $\lambda = \frac{v_{rotor}}{V} = \frac{\omega * d}{V}$ where V is the wind speed, ω is the angular velocity of the turbine, and d is the diameter of the semi-cylindrical blade.

The torque coefficient C_t is the ratio between the torque in the rotor and the theoretical torque that the wind can cause: The static torque coefficient C_{ts} expresses the turbine's ability to self-start. It is the ratio of the maximum static torque in the turbine and the theoretical wind torque:

$$C_{ts} = \frac{T_s}{T_w} = \frac{T}{\frac{1}{4} * \rho * A_s * d * V^2} \quad (I-2)$$

where T_s is the maximum static torque.

The torque in the rotor can be calculated using the following equation: $T = I * \alpha$, where I is the rotor's moment of inertia and α is the rotor's angular acceleration. The power coefficient C_p is the ratio of the extracted power from the wind to the available power in the wind:

$$C_p = \frac{P_{\omega}}{P_a} = \frac{T * \omega}{\frac{1}{2} * \rho * H * D * V^3} \quad (I-3)$$

Using these factors, we can learn about the turbine's characteristics and analyze its performance.

I.3.3.1 Two blades Vs. Three Blades

Experimental studies by confirm that H-Darrieus wind turbines do perform well at low to medium wind speeds (cut in speed at around 2.5 m/s). According to the same study, two blades perform better than three blades as more drag is wasted in the three blades versions. The power coefficient of the two blade design is higher than that of the three blade design.

This result is confirmed by . In their experimental study, they found that 2 blades do perform better than 3 blades. They also found that 4 blades perform even better than 2 blades at low tip speed ratio (TSR), and that 3 blades perform better at higher TSR[1].

I.4 Algeria wind speed Potential

Algeria present a good potential in term of wind Energy as shown in the study done before (**A contribution in the actualization of wind map of Algeria**) Whereas, it's explain the impact Wind Energy can prove in term of CO2 foot print .

This study has been recalibrate the wind Data that been published on 2004 especially in the region of Hassi Ramal and Laghaouat where there is an important wind field across this region considered to be 6 m/s annually, However, the conclusion of this study was used as reference for my study for the wind speed in **Ouargla** region[3].

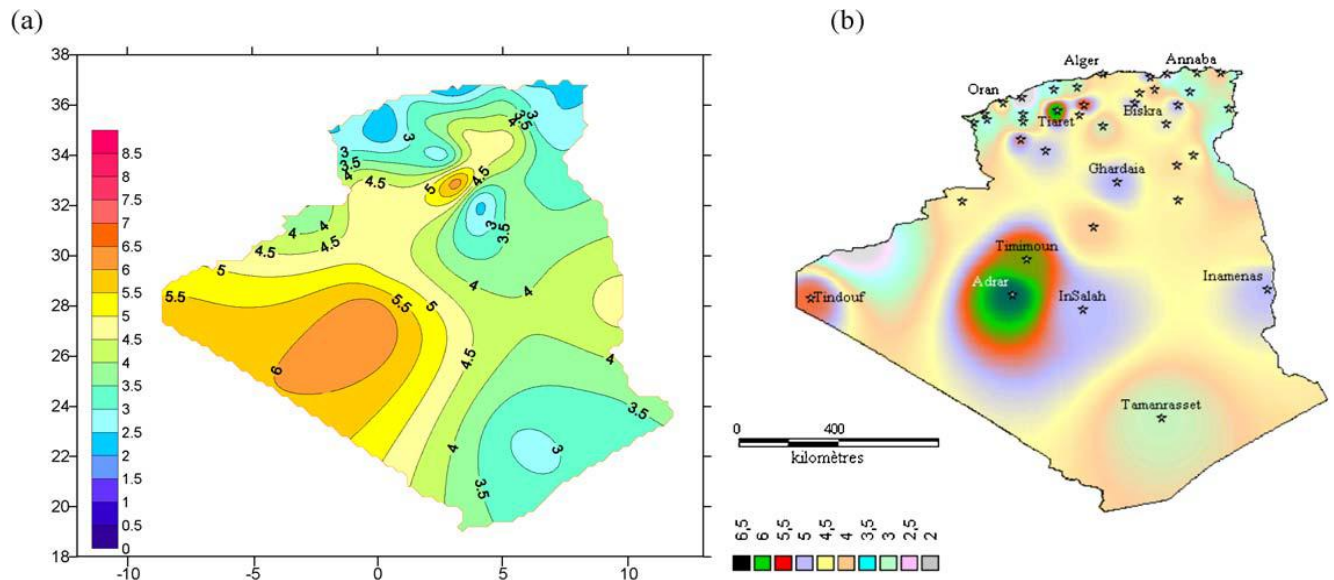


Figure I- 12: Annual maps of wind speed in Algeria at 10 m high.

1.5 Conclusion

Research and development on the new resource especially on wind energy continue to develop as the market is promising, there are increasing numbers of manufactures all over the world, where Large and small scale vertical and horizontal wind turbine been produced.

Chapter II

Mathematical Methodology

Chapter II

Mathematical Methodology

II.1 Introduction

In this chapter we will discuss the mathematical equations used to resolve a finite volume, ANSYS FLUENT can handle both steady-state and transient analyses, and has several different options for modeling turbulence. Conservation of both mass and momentum is solved in all fluid flow cases, and in compressible flow. Consider a control volume which encloses a specified mass of fluid in a steady state flow field. Also consider a control surface around this volume, through which a certain mass of fluid enters and exits over a specific interval of time. If the flow is steady-state, these quantities are equal; therefore, there is no change in mass of the volume. Moreover, we will discuss the governing equation for these phenomena and assumptions taken to simulate this rotor.

II.2 Equations Governing

The equations governing the problem are the continuity equations, which express the mass conservation, the momentum and Navier Stokes equations. For a simple formulation of the problem, we will suppose some assumption [10].

II.3 Assumptions

- The flow is in stationary (unsteady)-
- The flow is two-dimensional (since we will do numerical calculations in 2D, we will not take into account the variations of the flow in the vertical plane. On the other hand, we neglect the losses at the end of the blade. real, the effects of losses at the end of the blade are negligible if the blades are of considerable length compared to the diameter of the rotor)
- Fluid is Air incompressible.
- The fluid is viscous.
- No heat transfer.
- No Shear for the walls.
- No slip for the Airfoils

Given the above assumptions, the basic equations governing the flow are respectively presented as below:

II.3.1 Continuity Equation

$$\frac{\partial u}{\partial x} + \frac{\partial v}{\partial y} = 0 \quad (\text{II-1})$$

II.3.3 Equation of momentum following x

$$u \frac{\partial(u)}{\partial x} + v \frac{\partial(u)}{\partial y} = -\frac{1}{\rho} \frac{\partial p}{\partial x} + \nu \left(\frac{\partial^2 u}{\partial x^2} + \frac{\partial^2 u}{\partial y^2} \right) - \frac{\partial}{\partial y} \overline{U_1 U_2} \quad (\text{II-2})$$

II.3.3 Equation of momentum following Y

$$u \frac{\partial(v)}{\partial x} + v \frac{\partial(v)}{\partial y} = -\frac{1}{\rho} \frac{\partial p}{\partial y} + \nu \left(\frac{\partial^2 v}{\partial x^2} + \frac{\partial^2 v}{\partial y^2} \right) - \frac{\partial}{\partial y} \overline{U_2^2} \quad (\text{II-3})$$

II.4 The turbulence model

There are several models of closure. As the model $\mathbf{k}\text{-}\boldsymbol{\varepsilon}$ (STANDARD and REALIZABLE) in this study i use the turbulence module $\mathbf{k}\text{-}\boldsymbol{\varepsilon}$ STANDARD.

II.4.1 Model $\mathbf{k}\text{-}\boldsymbol{\varepsilon}$

It is a model with two transport equations for two turbulence parameters, using the analogy between momentum exchange by molecular interaction at the microscopic scale (viscous stresses) and the exchange of motion quantity by turbulence at the macroscopic scale (Reynolds constraints).

The idea of the model $\mathbf{k}\text{-}\boldsymbol{\varepsilon}$ is that it can be constructed from these quantities a (turbulent viscosity specific to the flow), or the turbulent viscosity is given by the following relation[10].

$$\mathbf{v}_{t=C_{\mu}}(\mathbf{k}^2/\boldsymbol{\varepsilon}) \quad (\text{II-4})$$

* \mathbf{c}_{μ} . is a dimensionless coefficient that must be evaluated experimentally

* \mathbf{K} : is The kinetic energy of turbulence defined by

$$k = \frac{1}{2} \overline{u_1'^2} = \frac{1}{2} (\overline{u_1'^2} + \overline{u_2'^2} + \overline{u_3'^2}) \quad (\text{II-5})$$

* ε : the dissipation rate of the kinetic energy turbulence k given by the following

$$\varepsilon = V \left[\frac{\partial u'}{\partial x_j} \right]^2 \quad (\text{II-6})$$

This dissipation term that appears in the equation of turbulent kinetic energy-remains to be determined. The typical length scale of the large structures of the turbulent L is deduced from:

$$\varepsilon = K^{1/2}/L \quad (\text{II-7})$$

The modeled equation of turbulent kinetic energy is written in the following semi-empirical form;

$$\frac{\partial k}{\partial t} + \overline{u_j} \frac{\partial k}{\partial x_j} = V_t \left(\frac{\partial \overline{u_i}}{\partial x_j} + \frac{\partial \overline{u_j}}{\partial x_i} \right) \frac{\partial \overline{u_i}}{\partial \overline{u_j}} + \frac{\partial}{\partial x_j} \left(\left(\frac{v}{\sigma_{k,l}} + \frac{v_t}{\sigma_{k,t}} \right) \frac{\partial k}{\partial x_j} \right) - \varepsilon \quad (\text{II-8})$$

(I) (II) (III) (IV)

* The terms of Equation (II.8) are referred to as follows:

- (I): Represents the rate of variation of kinetic energy K
- (II): Represents diffusion transport of kinetic energy.
- (III): Represents the shear production of the turbulent kinetic energy.
- (IV): Represents the dissipation of turbulent kinetic energy K .

II.4.1.1 Modeled equation of ε :

The modeled form of the kinetic energy dissipation rate transport equation is expressed.

$$\frac{\partial \varepsilon}{\partial t} + \overline{u_j} \frac{\partial \varepsilon}{\partial x_j} = \underbrace{C_{\varepsilon 1}}_{\text{(I)}} \frac{\varepsilon}{k} V_t \underbrace{\left(\frac{\partial \overline{u_1}}{\partial x_j} + \frac{\partial \overline{u_1}}{\partial x_j} \right)}_{\text{(II)}} \frac{\partial \overline{u_1}}{\partial x_j} + \underbrace{\frac{\partial}{\partial x_j} \left[\left(\frac{v}{\sigma_{\varepsilon,t}} + \frac{v_t}{\sigma_{\varepsilon,t}} \right) \frac{\partial \varepsilon}{\partial x_j} \right]}_{\text{(III)}} - \underbrace{C_{\varepsilon 2} \frac{\varepsilon^2}{K}}_{\text{(IV)}} \quad \text{(II-9)}$$

The terms of equation (II-9) are:

- **(I):** Represents the rate of change ε
- **(II):** Represents the production rate (source) of ε -2
- **(III):** Represents diffusion transport of the dissipation of turbulent energy.
- **(IV):** Represents the dissipation (well) of ε

II.4.1.2 Models of constants

To make the system of equations operational we adopt the standard constants of the model given by Laufer and Spalding (1974). They are gathered in the following table:

Table II- 1: Coefficients of standard K- ε Model

c_μ	$C_{\varepsilon 1}$	$C_{\varepsilon 3}$	Σk	$\Sigma \varepsilon$
0.09	1.44	1.92	1.0	1.0

II.4.1.3 Mach Number

The number of a Mach is a dimensionless number, Marked Ma, which expresses the ratio of the local speed of a fluid to the speed of sound in the same fluid. Which change over the nature and temperature of the fluid[10].

$$\mathbf{Ma} = \mathbf{V} / \mathbf{C} \quad \text{(II-10)}$$

The compressibility of the air can be neglected for Mach numbers less than about 0.3. The sonic case defined above as the boundary between the subsonic and the supersonic has no physical reality: it is replaced by a wide transition zone, in which the phenomena's are particularly complicated.

The equation of state allows to rewrite it according to the specific gas constant R_s (287 / J / Kg / K for the area) and the temperature T in Kelvin.

$$C = \sqrt{\gamma R_s T} \quad (\text{II-11})$$

II.4.2 SST k-omega turbulence model

Shear-stress transport (SST) k-omega turbulence model is a type of hybrid model, combining two models in order to calculate flow in the near-wall region. It was designed in response to the problem of the k-epsilon model's unsatisfactory near-wall performance for boundary layers with adverse pressure gradients. It uses a standard k- ϵ model to obtain flow properties in the free-stream (turbulent) flow region far from the wall, while using a modified k- ϵ model near the wall using the turbulence frequency ω as a second variable instead of turbulent kinetic energy dissipation term ϵ . The transport equation for turbulent kinetic energy k for the k- ω model is:

$$\begin{aligned} \frac{\partial}{\partial t}(\rho k) + \frac{\partial}{\partial x_j}(\rho k u_j) &= \frac{\partial}{\partial x_j} \left[\left(\mu + \frac{\mu_t}{\sigma_k} \right) \text{grad}(k) \right] + P_k - \beta^* \rho k \omega \end{aligned} \quad (\text{II-12})$$

(I) (II) (III) (IV) (V)

Where

$$P_k = \left(2\mu_t \frac{\partial u_i}{\partial x_j} \cdot \frac{\partial u_j}{\partial x_i} - \frac{2}{3} \rho k \frac{\partial u_i}{\partial x_j} \delta_{ij} \right) \quad (\text{II-13})$$

Table II- 2: Equation terms definition

(I)	Transient term	Accumulation of k (rate of change of k)
(II)	Convective transport	Transport of k by convection
(III)	Diffusive transport	Turbulent diffusion transport of k
(IV)	Production term	Rate of production of k
(V)	Dissipation	Rate of dissipation of k

σ_k And β^* are equation constants

The transport equation for turbulent frequency ω for the k- ω model is:

$$\begin{aligned} \frac{\partial}{\partial t}(\rho \omega) + \frac{\partial}{\partial x_i}(\rho U_i \omega) &= \frac{\partial}{\partial x_i} \left[\left(\mu + \frac{\mu_t}{\sigma_{\omega,1}} \right) \text{grad}(\omega) \right] + \gamma_2 \left(2\rho_t \frac{\partial u_i}{\partial x_j} \cdot \frac{\partial u_i}{\partial x_j} - \frac{2}{3} \rho \omega \frac{\partial u_i}{\partial x_j} \delta_{ij} \right) - \beta_2 \rho \omega^2 + 2 \frac{\rho}{\sigma_{\omega,2} \omega} \frac{\partial k}{\partial x_k} \frac{\partial \omega}{\partial x_k} \end{aligned} \quad (\text{II-14})$$

(I) (II) (III) (IV) (V) (VI)

The general description for each of the terms in Equation (I) to (V) are the usual terms for accumulation, convection, diffusion, production, and dissipation of u . Last term (VI) is called a ‘**cross diffusion**’ term, an additional source term, and has a role in the transition of the modeling from ε to ω [2].

II.4.3 Turbulence Intensity

The turbulence intensity, I , is defined as the ratio of the root-mean-square of the velocity fluctuations, u' , to the mean flow velocity, u_{avg} .

A turbulence intensity of 1% or less is generally considered low and turbulence intensities greater than 10% are considered high. Ideally, you will have a good estimate of the turbulence intensity at the inlet boundary from external, measured data. For example, if you are simulating a wind-tunnel experiment, the turbulence intensity in the free stream is usually available from the tunnel characteristics. In modern low-turbulence wind tunnels, the free-stream turbulence intensity may be as low as 0.05%.

For internal flows, the turbulence intensity at the inlets is totally dependent on the upstream history of the flow. If the flow upstream is under-developed and undisturbed, you can use a low turbulence intensity. If the flow is fully developed, the turbulence intensity may be as high as a few percent. The turbulence intensity at the core of a fully-developed duct flow can be estimated from the following formula derived from an empirical correlation for pipe flows [11].

$$I \equiv \frac{u'}{u_{avg}} = 0.16(Re_{D_H})^{-1/8} \quad \text{(II-15)}$$

II.5 Number of Reynolds

The Reynolds number represents the ratio between the inertial forces and the viscous forces.

This dimensionless number appears naturally by sizing the Navier - Stokes equations. We define it in the following way:

$$Re = \frac{UL}{\nu} \quad (\text{II-16})$$

Where $\nu = \mu/\rho$ is the kinematic viscosity of the fluid. The characteristic length L is the diameter of a pipe, or the dimension of an obstacle[11].

- RE <2000: laminar flow
- RE <4000: turbulent flow
- For 2000 <Re <4000, we observe a transition regime.

II.6 Conclusion

The continuity and momentum was used for this project including the turbulence model K- ϵ and the intensity of the turbulent was used as well. This equation was the sour of the solver **Fluent** integrated on **ANSYS** to resolve the unsteady flow through our H- Darrieus vertical wind turbine in merge of the sliding mesh technic.

Chapter III
***Design Optimization and
Setup***

Chapter III

Design optimization and Setup

III.1 Introduction

In this chapter we will discuss the design criteria and parameters that being used to optimize the H-Darrieus wind turbine and define the optimum 2D dimensions for the wind velocity for Ouargla region, after defining the optimum dimensions which than will be used as inputs for the CFD simulation by using ANSYS 18.2, Moreover, we will discuss the important steps for designing, then Meshing and using Fluent to resolve the unsteady slide and Mesh technic for the proposed wind field from other study being used as reference.

III.2 Designing and Optimization of VAWT

Many factors could help in optimizing and designing the best possible wind turbine, thus factors are Presented in the workflow below

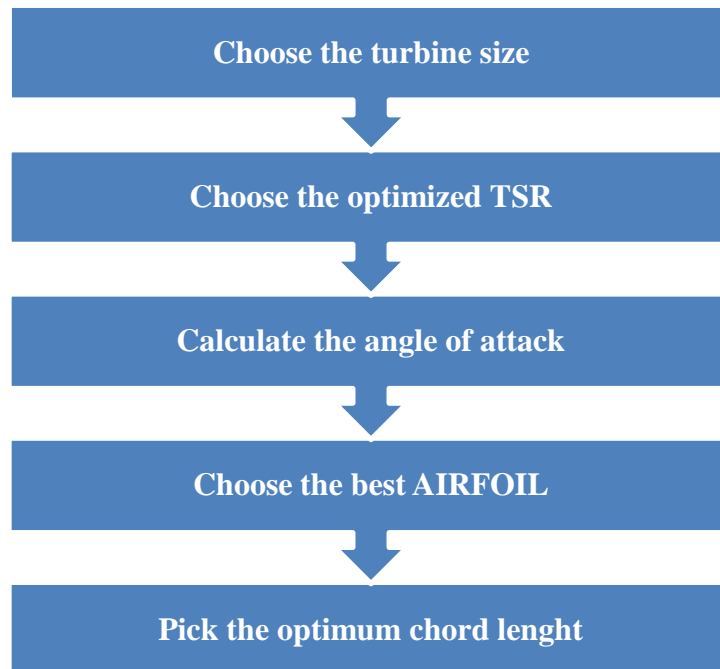


Figure III- 1: Design optimization work flow

III.2.1 Choose the turbine size

The area of the wind turbine is presented on the power coefficient equation (III-1), I calculate the area of the desired VAWT dimension by assuming a power coefficient of 0.45 with a different wind speed of **Ouargla** and then I choose the optimum size for our case, the calculation and the results are presented on the table below

$$C_p = \frac{P_w}{P_a} = \frac{T \cdot w}{\frac{1}{2} \rho \cdot D \cdot H \cdot V^3} \quad (\text{III-1})$$

From this equation I explore the Area of wind turbine As $A = D \cdot H$ The rotor dimension and area of study presented on the below table

Table III- 1 Ouargla Wind Speed

Ouargla wind speed (m/s)	Calculated area (m ²)	Turbine size (D*H) (m*m)
High (4.9)	1	1*1
Average (3.8)	2	2*1
Low (2.8)	5	2.5*2

Note: the above wind speed data was extracted from a technical paper [1]

The table III-1 explains the interaction between the wind speed and the size of the turbine, by mean as the wind speed increases the area decrease by calculation. The required wind velocity for a small scale wind turbine will be low in order to generate the same power.

Looking at table-1 at the average annual wind speed of 3.8 m/s for **Ouargla** we can conclude the optimum size presented by the (D: Diameter, H: Height) of our case as explained in fig III-2 below

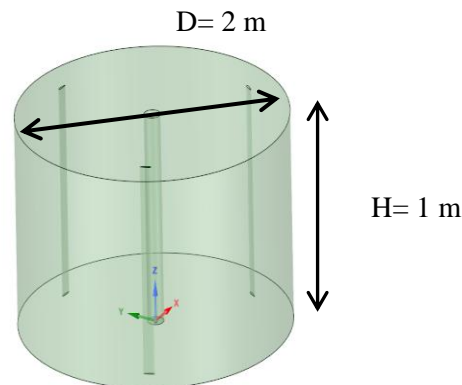


Figure III- 2 The optimized turbine size on 3D

III.2.2 Choose the optimized Tip Speed Ratio (TSR)

TSR defined as the ratio between the tangential speed at blade tip and the actual wind speed. The TSR is expressed as below

$$TSR = \frac{\omega * r}{v_w} = \frac{\pi * N * D}{60 * v_w} \quad (III-2)$$

Where ω is the angular speed [rad/s], r the rotor radius [m], v_w the ambient wind speed [m/s] and N the number of rotation per minutes [Round/ min], Furthermore the optimal TSR for a H-Darrieus wind turbine as described in Chapter 01 fig-3, the optimum TSR for our

$$TSR = 6$$

III.2.3 Calculate the optimal angle of Attack

The angle of attack of the Airfoil trajectory play in important rule in the lift and drag ration (Cl/Cd), However, in order to obtain the optimum angle of attach we need to calculate the Reynolds number for our case and then we can extract the angle of attack.

$$Re = \frac{\rho * v * l}{\mu} = \frac{v * l}{\vartheta} \quad (III-3)$$

Where:

ρ : The air density (1.22 kg/m³)

v : The wind speed (3.8 m/s)

l : The intial chord length of the airfoil (0.1 m)

ϑ : The Kinematic viscosity of the air (1.511E-5 m²/s @20degC)

μ : The dynamic viscosity of the air.

$$Re = \frac{3.8 * 0.1}{1.511E - 5} = 25148$$

By using a software called JavaFoil we can check the optimum angle of attack for a different Re number for a specific Airfoil profile, the below fig explain how the lift and drag ratio change over (-20 to 20 deg) angle of attack for a two number of Reynolds (25.000 and 100.000).

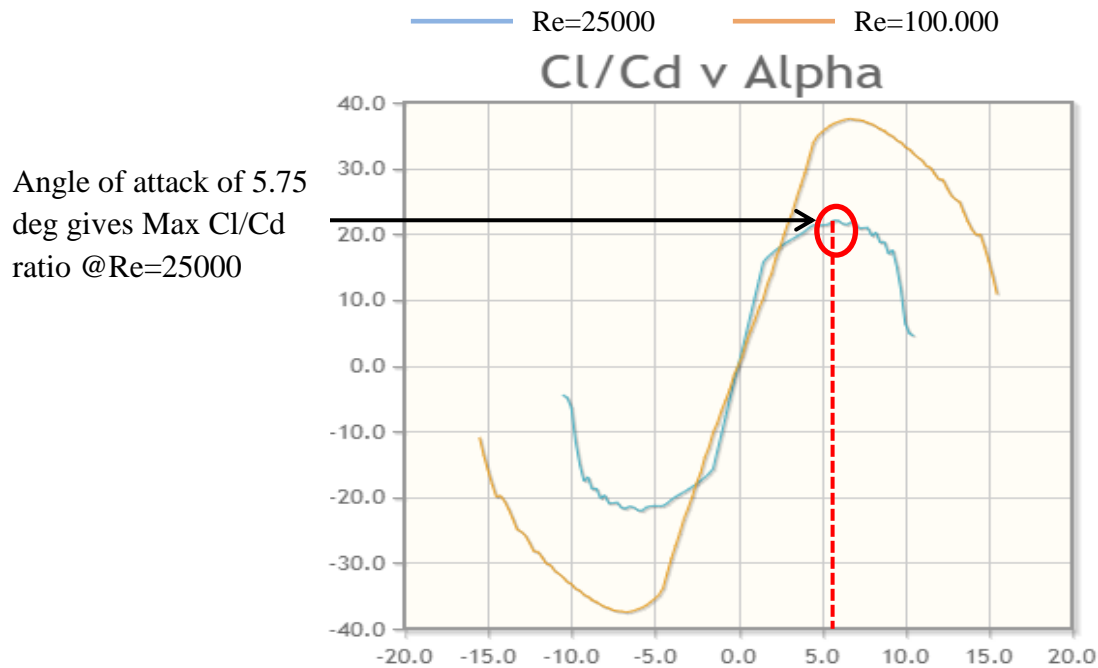


Figure III- 3:Cl/Cd ratio for various Angle of Attack

The fig 2 gives an maximum lift to drag ratio equal to 21 at 5.75 deg angle of Attack, therefore, The airfoil of the designed vertical wind turbine will be tilted with 5.75 deg[13].

$$\alpha_{\text{optimum}} = 5.75 \text{ deg}$$

III.2.4 Choose the best AIRFOIL

The 2D airfoil profile and dimension has an important rule on increasing or decreasing the lift/ drag ration and hence the power coefficient.

CFD analysis for H-Darrieus turbine as low speed wind energy converter is a technical study where it shows that NACA0018 could be one of the best profile due to the generated lift force over the drag, For that propose I run a several airfoil profile using an airfoil tool available on the internet <http://airfoiltools.com> in order to check the best suitable 2D profile for our case. Three airfoil profiles (NACA0018, NACA0021 and NACA0010-35) were compared and presented on Fig III-4 and 5 [13].

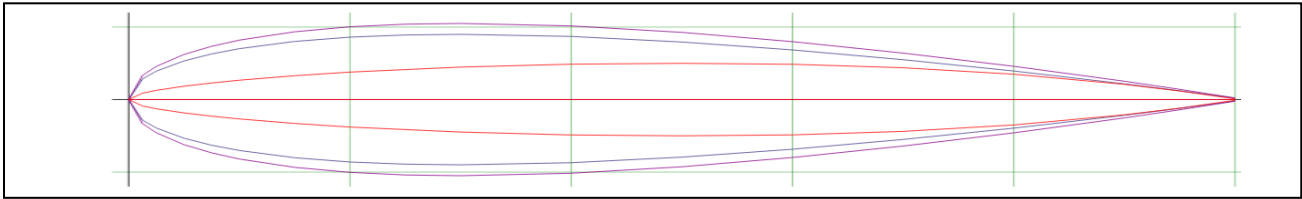


Figure III- 4: Proposed Airfoil profiles

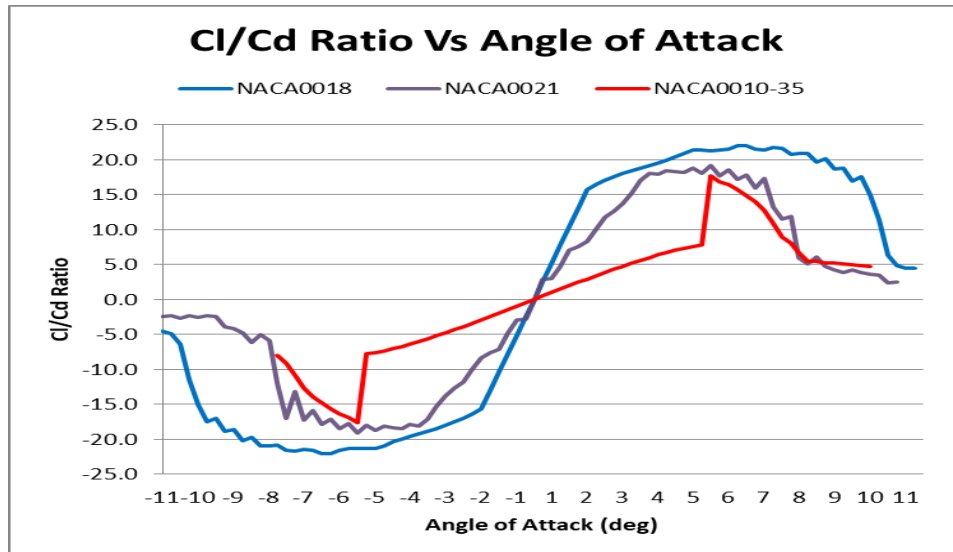


Figure III- 5: lift to drag ratio for different airfoil profile

From the above Fig.4 the airfoil profile NACA 0018 in blue presented the maximum lift/ Drag ratio comparing to other profiles, therefore, **NACA0018** is selected as the blade profile for our case.

The chord is the length between leading edge and trailing edge of the blade profile. NACA0018 present the following parameters[13].

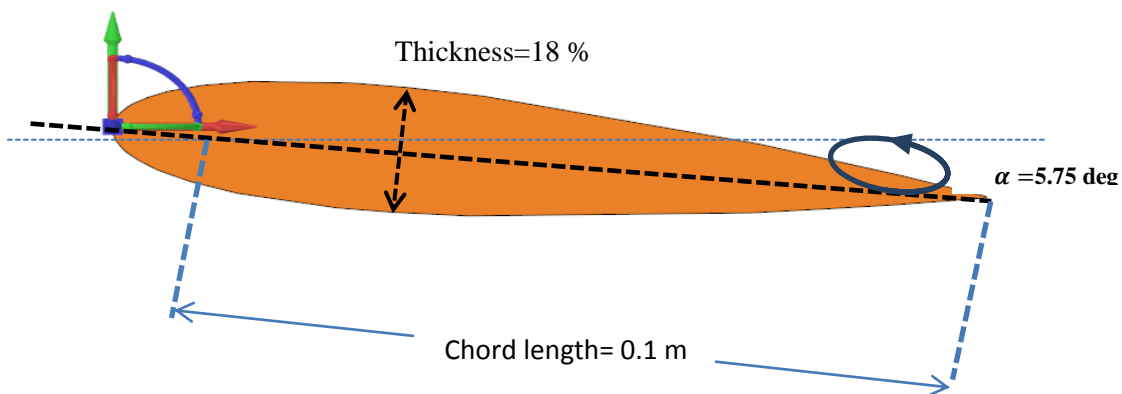


Figure III- 6: NACA0018 profile and characteristics

III.3 Simulation and Setup using ANSYS 18.2

III.3.1 ANSYS Overview

ANSYS Workbench combines the strength of our core simulation tools with the tools necessary to manage your projects. You will work with your ANSYS Workbench project on the main project workspace, called the Project tab. To build an analysis, you add building blocks called systems to the Project Schematic. These systems make up a flowchart-like diagram that represent the data flow through your project. Each system is a block of one or more components called cells, which represent the sequential steps necessary for the specific type of analysis. Once you have added your systems, you can link them together to share and/or transfer data between systems.

ANSYS: Fluent. It “contains the broad physical modeling capabilities needed to model flow, turbulence, heat transfer, and reactions for industrial applications [...] Fluent covers a broad reach, including special models with capabilities to model in-cylinder combustion, aero-acoustics, turbo machinery and multiphase systems”[11].

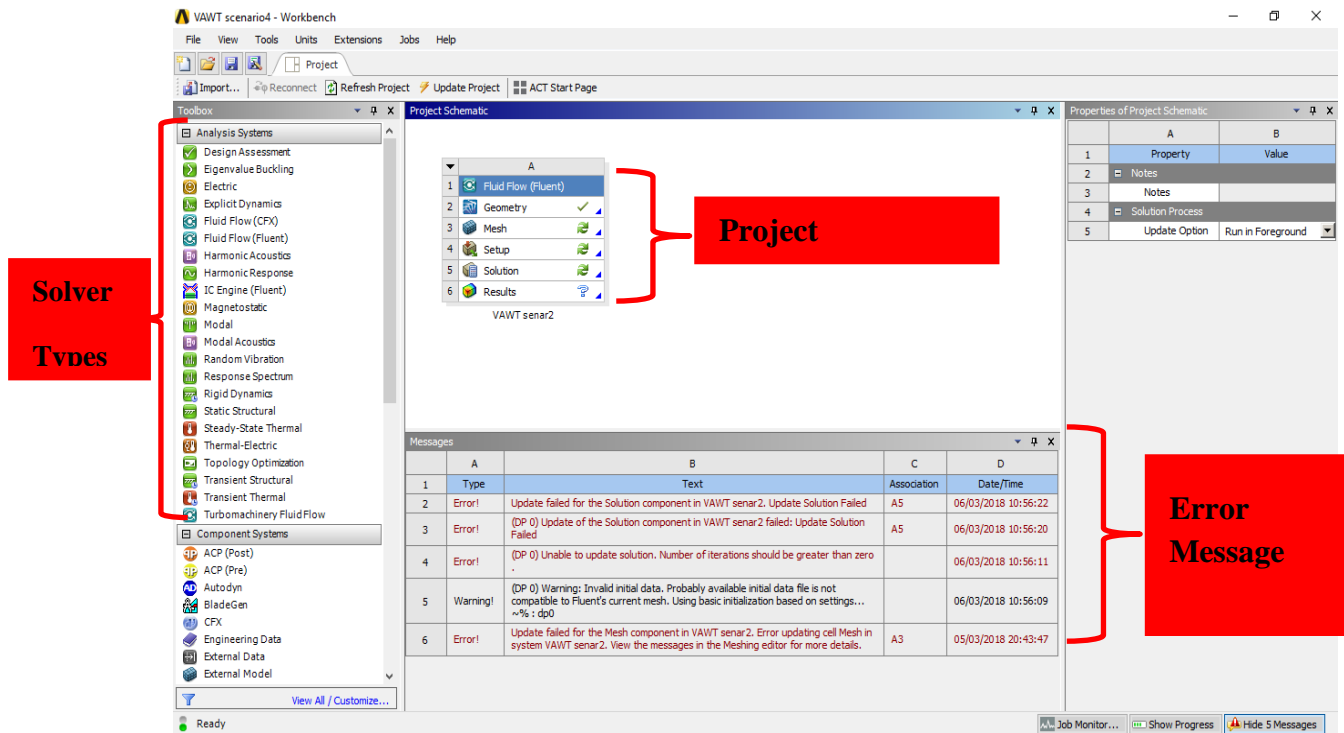


Figure III- 7:ANSYS Workbench windows overview

III.3.2 ANSYS WorkFlow

As mention in the overview the project workbench present the workflow needed to stimulate which ever domain (Heat Transfer, Aerodynamic, Acoustics....)[11].

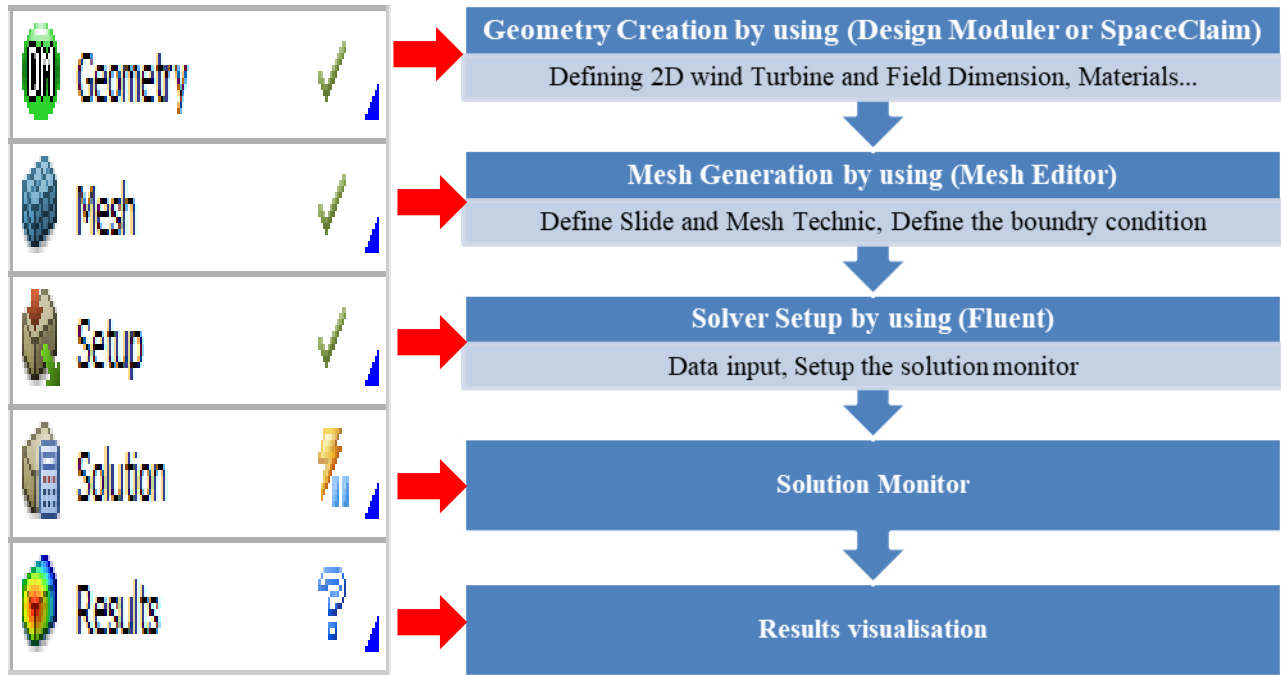


Figure III- 8:ANSYS Workflow description

III.3.2.1 Creating Geometry using Design Modular

The field of study is the 2D area where H-Darrieus wind turbine will be exposed to the wind velocity in order to test the turbine performance, it's containing two main domains, Fixed domain and rotating domain [2].

1. **The rotating domain** is the designed wind turbine and airfoils, the interface will be **1.25D** of the designed Diameter.
2. **The fixed domain** is the 2D test area where the turbine will be exposed to the wind speed, it's containing the following (Walls, velocity inlet and Pressure outlet), the area is a rectangle with **25Dx10D** of the designed Rotor Diameter.

The table and figure below present the Geometrical field of study which has been imported into the Design Modular software.

Table III- 2: Main geometrical features of the analysed rotor

Denomination	Value
Rotor Diameter (m)	2
Rotating zone diameter (m)	2.5
Rotor height (m)	1
Study wind area m ²	50 m X 20 m
Velocity Inlet (m/s)	3.8
Pressure Outlet (Pa)	0
Blade Type	NACA0018
Blade Chord (mm)	100
Thickness (%)	18
Number of Blades (initial)	3
Angle of Attack(deg)	5.75

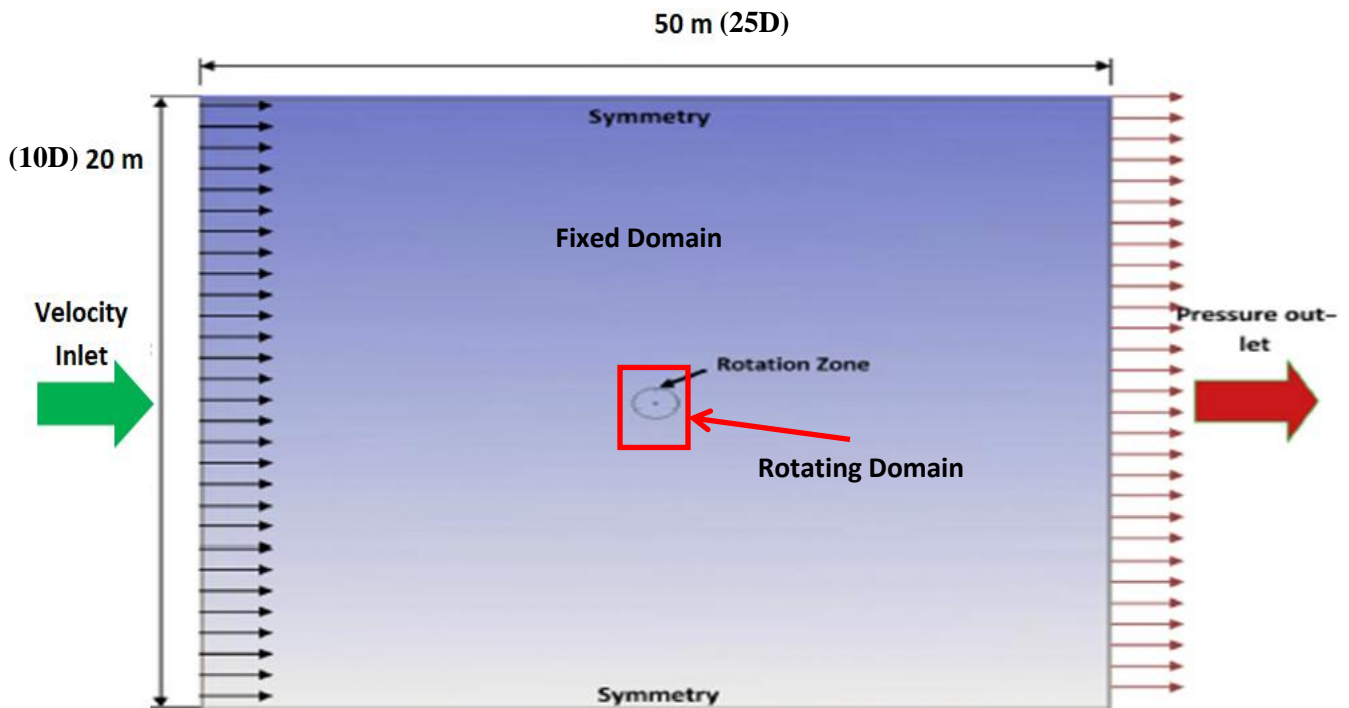


Figure III- 9: Geometrical dimension of the field study

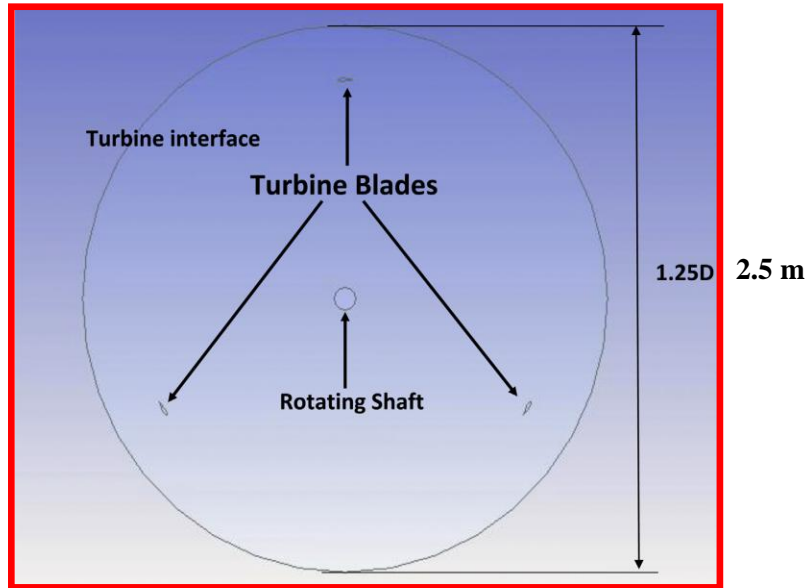


Figure III- 10:Schema of Rotating Domain

III.3.2.1.1 1st Step: Creating a Project file in ANSYS Workbench

Go to ANSYS Workbench, then Drag **Fluid Flow** in the Analysis system into project Schematic and name the project (VAWT) as below

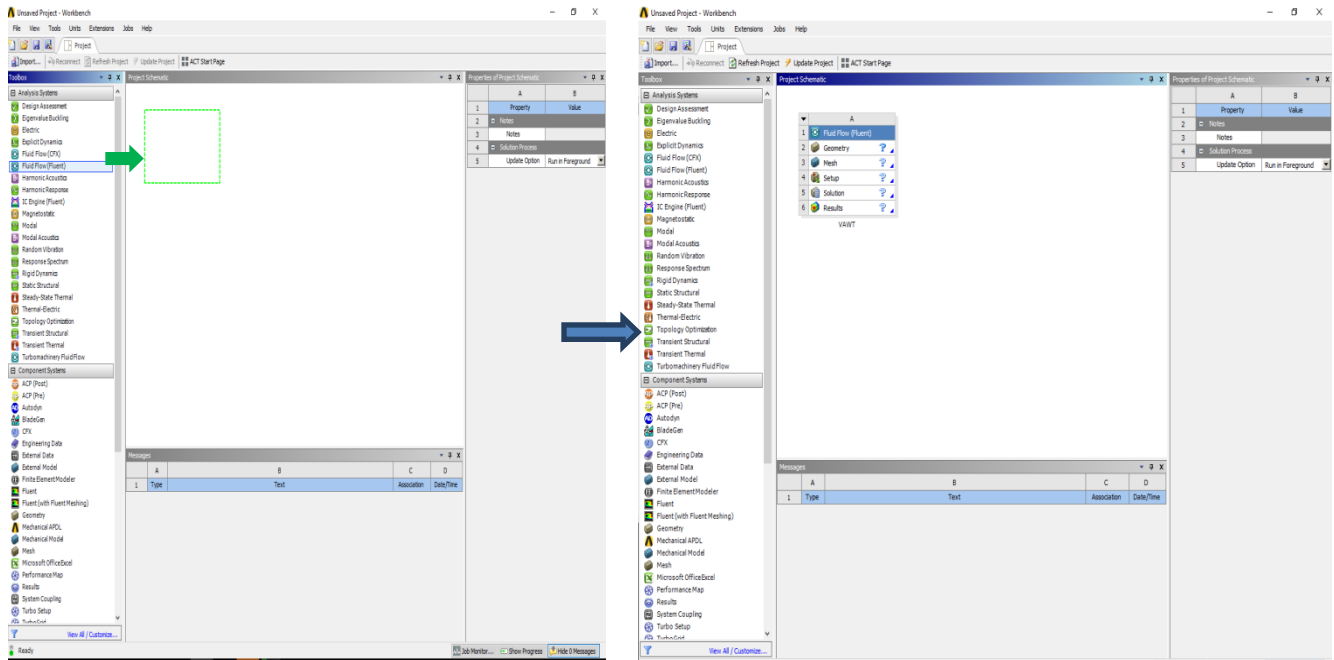


Figure III- 11:Creating a Project Flow in ANSYS Workbench

III.3.2.1.2 2nd Step: Creating the Geometry

After downloading NACA0018 profile Data from the web site <http://airfoiltools.com>, The airfoil data then open the first cell in the project file created before in Step 1. There are two softwares available **SpaceClaim** and **Design Moduler** which ever suitable can be used. In Our case I used SpaceClaim.

SpaceClaim\Open File\ select the .txt* file

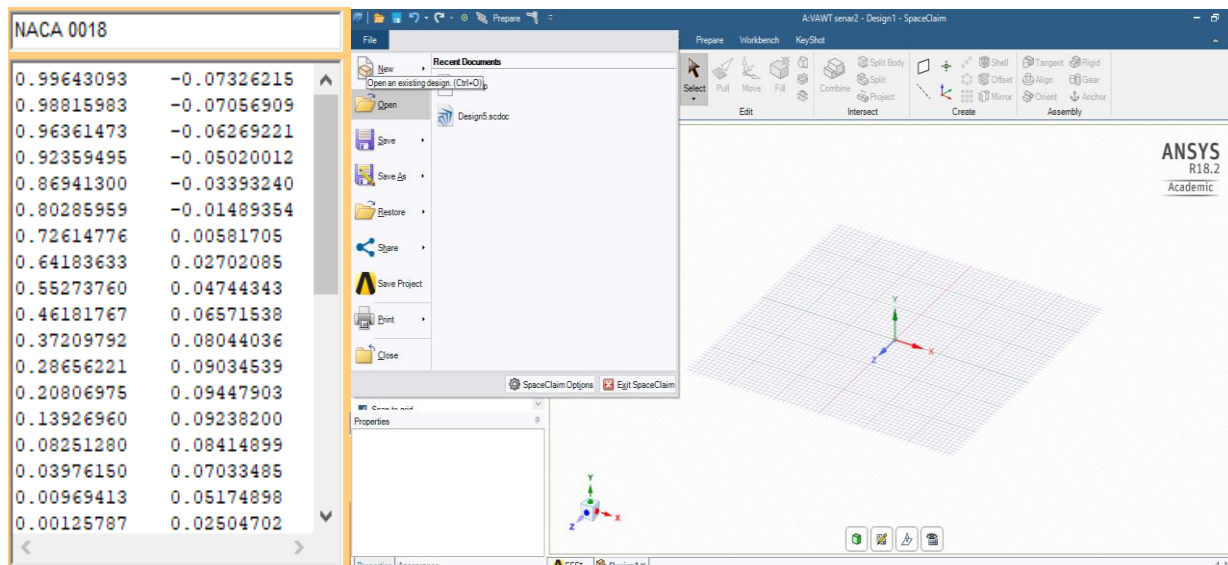


Figure III- 12:Importing Airfoil Data into SpaceClaim

- a) Create the first Airfoil profile then rotate it with the optimum Angle of Attack **5.75**

Go to Design\Move and Select the Airfoil then rotate it with 5.75 deg

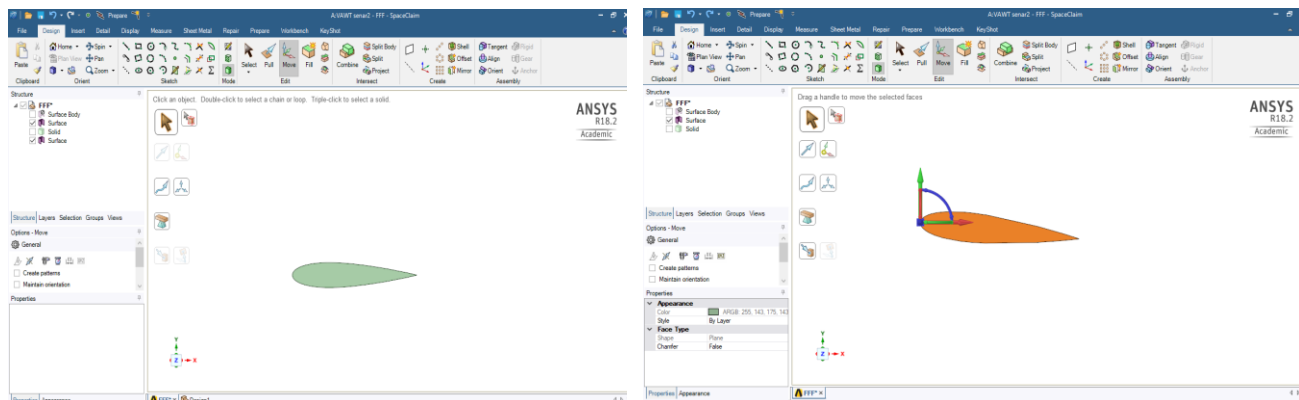


Figure III- 13:Creating NACA0018 profile with the Angle of Attack

b) Move the created Airfoil from in XY by $R= 1 \text{ m}$

Go to Design\ Move\ select the Airfoil and drag it 1 m away from the XY

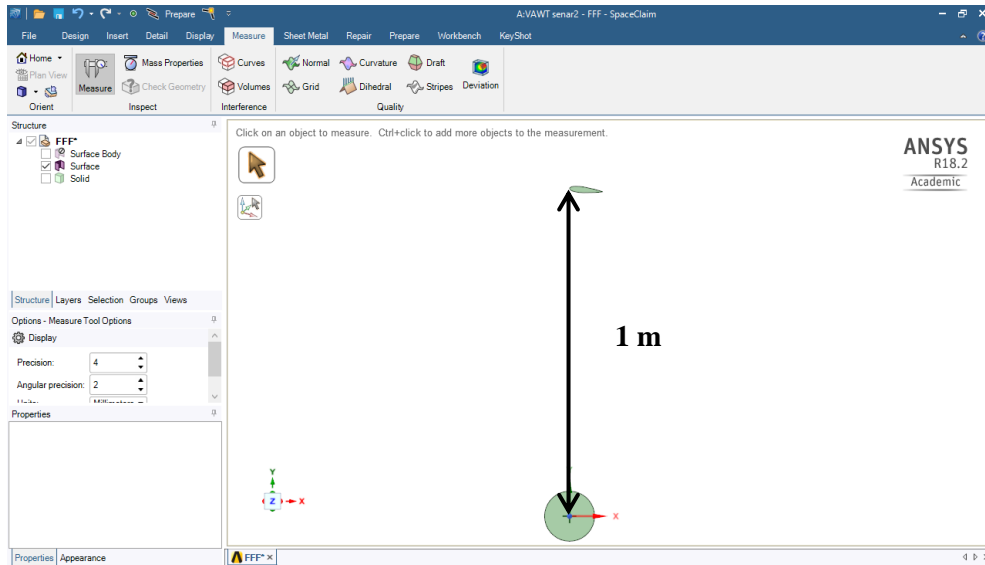


Figure III- 14:Move the blade by $R=1 \text{ m}$

c) Creating a 3 Airfoils

Go to Design/ create a circular Pattern then select the airfoil surface and chose the Axe Z, Set the number of blades to 3 blades in 360 deg.

Inputting a circular Pattern Data

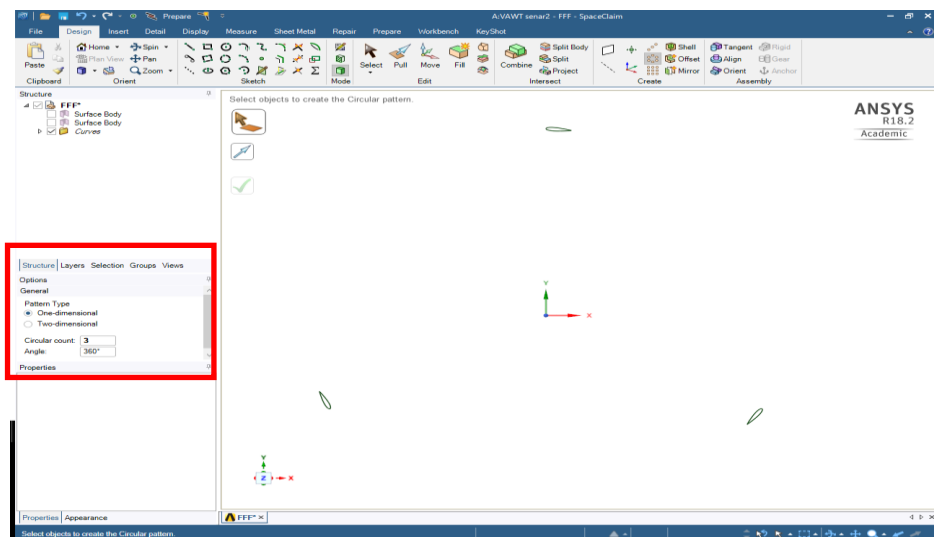


Figure III- 15:Creating a 3 Airfoil using a Circular Pattern

d) Creating a Rotating Domain

The rotating Domain as explained before is circle with 2.5 m diameter.

Go to Design/Sketch/ Create a Circle with a **D= 2.5 m**

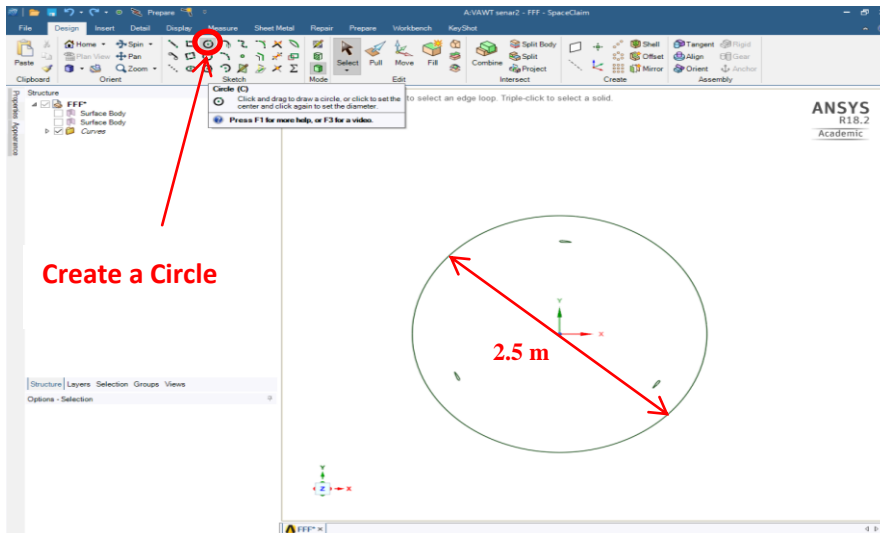


Figure III- 16:Create a Rotating Domain

e) Creating a Fixed Domain

As mention before is a rectangle with **50x20 m** dimension. Go to Design/Sketch/ create a rectangle

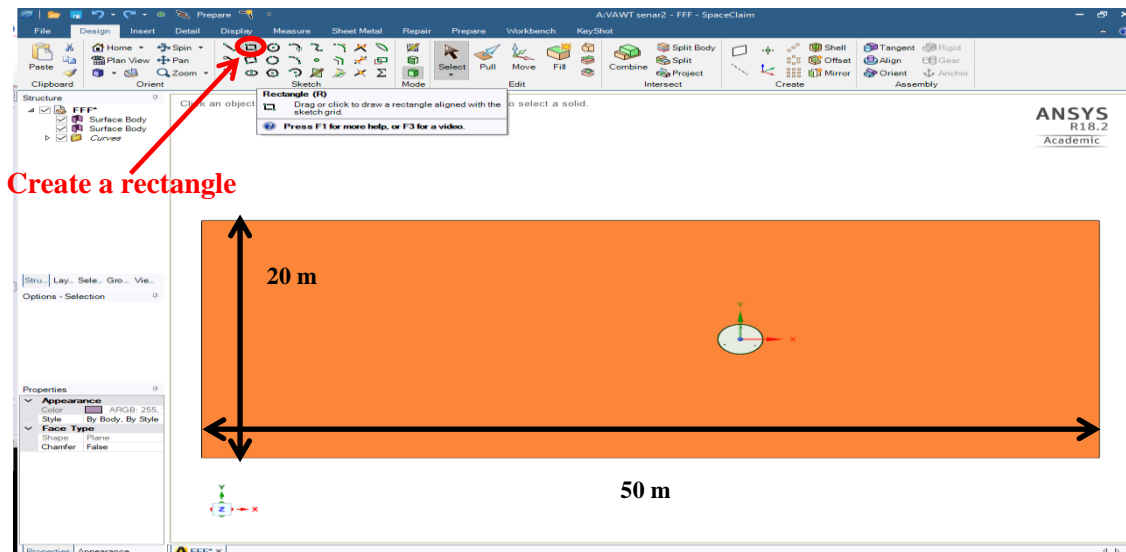


Figure III- 17:Creating a Fixed Domain

Once the Fixed and Rotating domains are created the Geometry is completed and ready to be exported for meshing. Save the Geometry file and close SpaceClaim then go to Mesh Editor.

III.3.2.2 Creating Mesh (3rd Step)

After importing the Data into Mesh Editor, we have to check the poor quality of the mesh without changing anything, for that go to **Generate Mesh**.

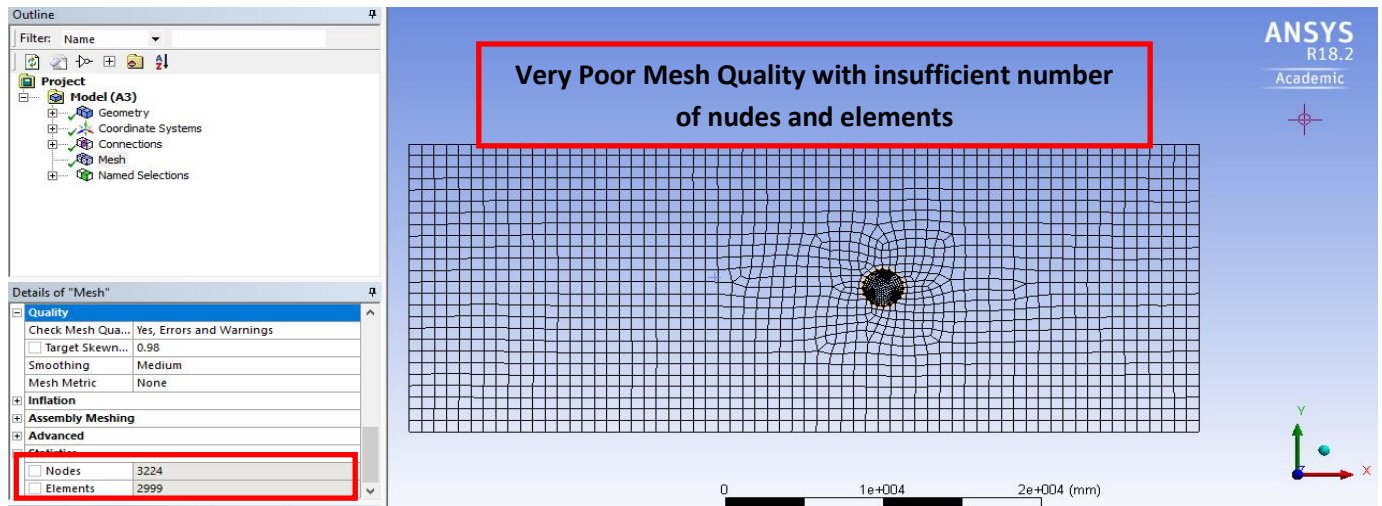


Figure III- 18: Mesh Quality check

III.3.2.2.1 Fixed Domain (Edge Sizing 1)

Choose the two Edges corresponding to (Inlet and Outlet) as described in the figure below. Go to Mesh\Right click and select Edge Sizing and choose the inlet+Outlet edges. Input the below Data

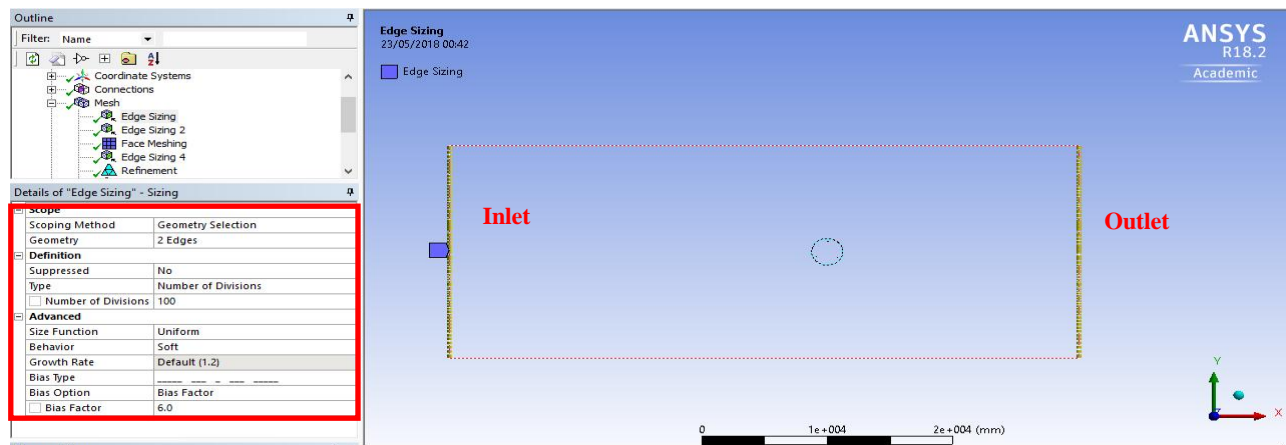


Figure III- 19:Edge Sizing 1

III.3.2.2.2 Fixed Domain (Edge Sizing 2)

Choose the two Edges corresponding to (Walls) as described in the figure below. Go to Mesh\Right click and select Edge Sizing and choose the wall edges. Input the below Data

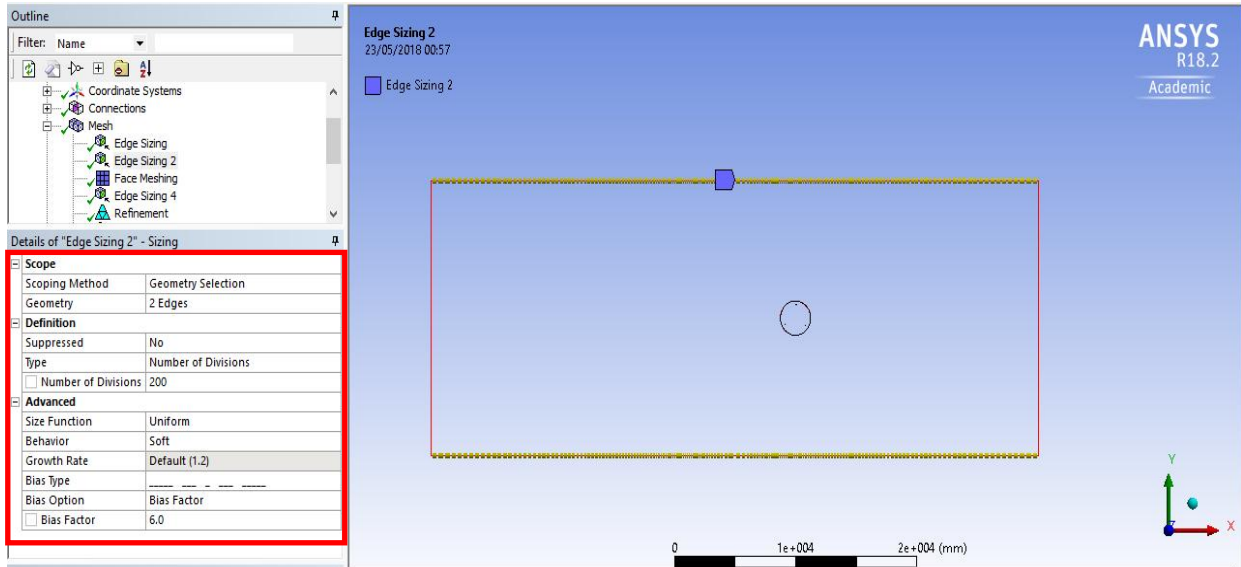


Figure III- 20:Edge sizing 2

III.3.2.2.3 Fixed Domain: Face Meshing

Go to Mesh\Right click and select Face Meshing. Select the Face and input the below Data

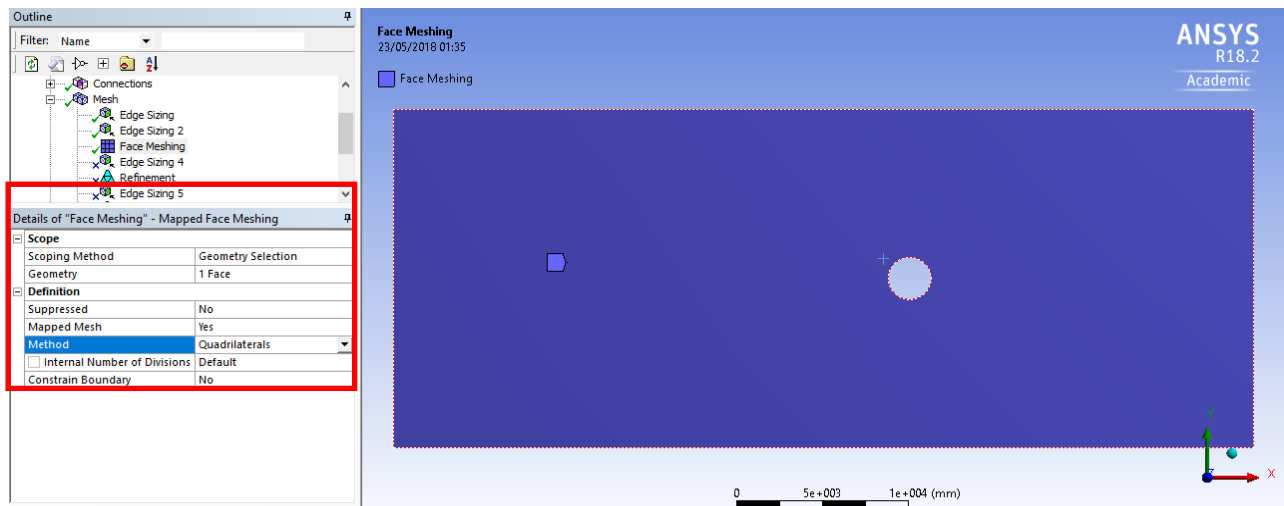


Figure III- 21:Face Meshing

The below table summarizes Fixed Domain Data input

Table III- 3: Fixed Domain Mesh Data Summary

Details	Edge Sizing 1	Edge Sizing 2	Face Meshing
Scoping Method	Geometry Selection	Geometry Selection	Geometry Selection
Geometry	Inlet and Outlet	2 Walls	Fixed Domain face
Types	Number of Divisions	Number of Divisions	Quadrilaterals
Number of Divisions	100	200	Default
Size function	Uniform	Uniform	-
Behavior	Soft	Soft	-
Growth Rate	Default(1.2)	Default(1.2)	-
Bias factor	6.0	6.0	-
Total Nodes	68072		
Total Elements	67536		

After inputting the above Data for Fixed Domain Meshing, Go to Generate Mesh. Mesh appears as below (Total of 68072 Node and 67536 Elements)

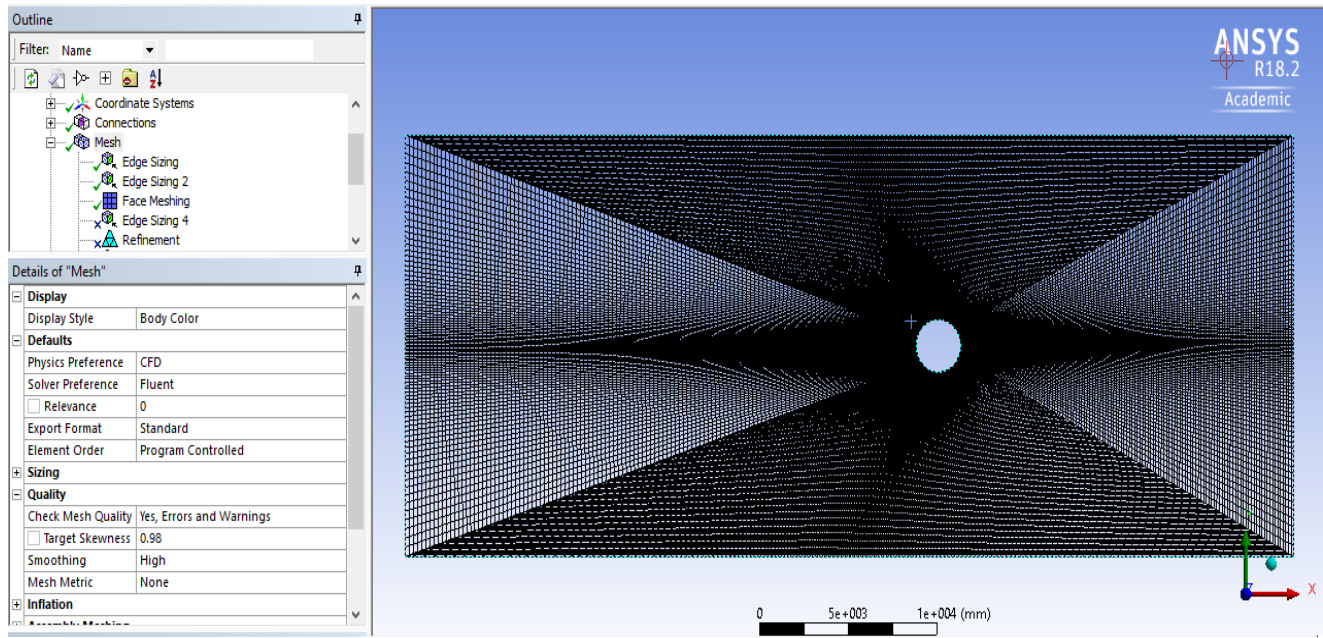


Figure III- 22:Fixed Domain Mesh Generation

III.3.2.2.4 Meshing Rotating Domain:

a- Meshing the Airfoils

The Airfoils section presented by **Edge Sizing 4, 5 and 6** required an intensive mesh in order to best simulate the CFD flow around the turbine section, therefore, The blades section was exposed into Edge sizing and refinement for the 3 blades as shown in the below figure

Edge Sizing: Go to Mesh\right click and choose the Edge sizing\Select edges one by one

Refinement: Go to Mesh \right click and choose the Edge sizing\Select edges one by one

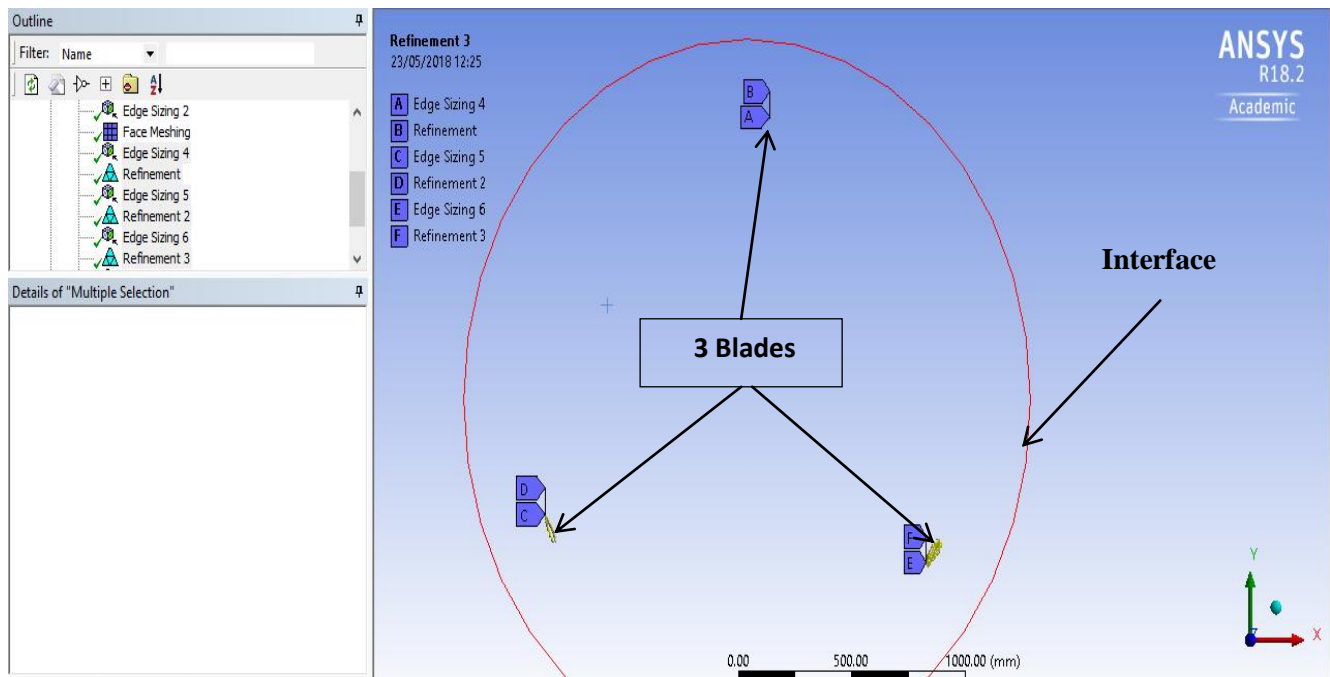


Figure III- 23:Meshing the Airfoils

b- Meshing the Interface

The Edge 7 present in Edge Sizing 7 is the interface between the rotating and fixed Domains, As explained in the sliding mesh technic is an important interface where the quality of the mesh need to be sufficient as shown the below figure

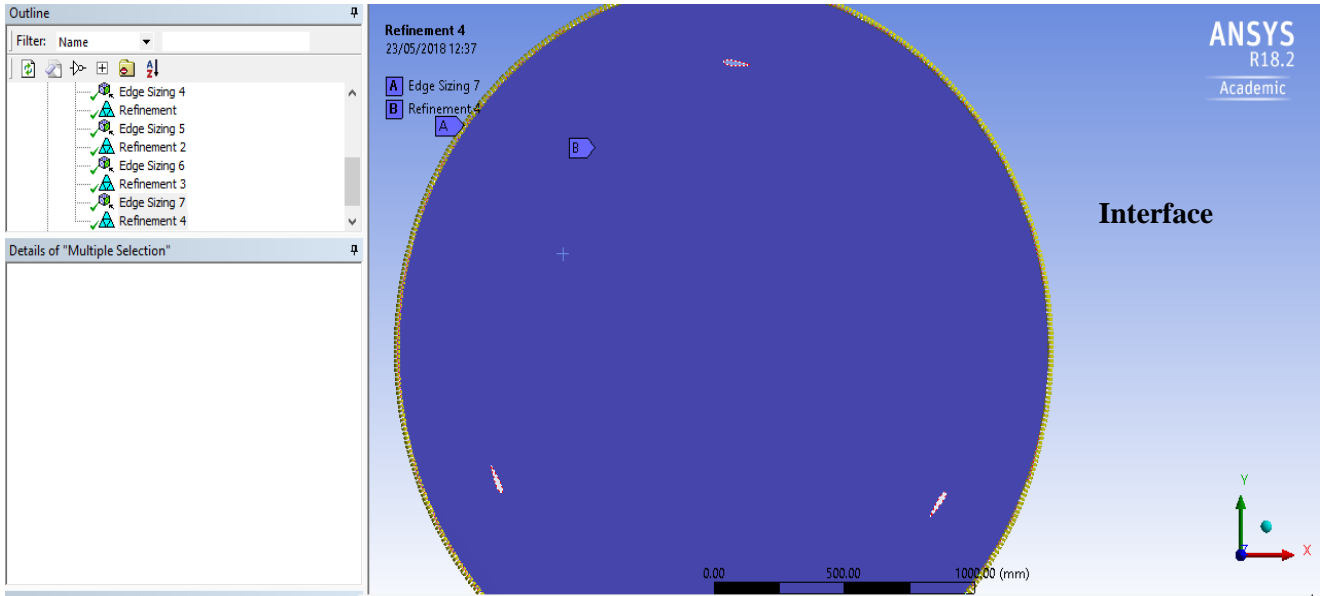


Figure III- 24:Meshing the Interface

The below table summarizes the Rotating Domain Data input

Table III- 4:Rotating Domain Mesh Data Summary

Details	Edge Sizing 4	Edge Sizing 5	Edge Sizing 5	Edge Sizing 7
Scoping Method	Geometry Selection			
Geometry	Airfoil 1	Airfoil 2	Airfoil 3	Interface
Types	Number of Divisions			
Number of Divisions	50	50	50	500
Size function	Uniform			
Behavior	Hard	Hard	Hard	Soft
Growth Rate	-	-	-	Default (1.2)
Refinement	2	2	2	3
Total Nodes	157373			
Total Elements	155262			

The Table III-4 shows a number of Nodes for the rotating domain greater than the Fixed Domain due to the importance of this area and the presence of multiple edges interact in between.

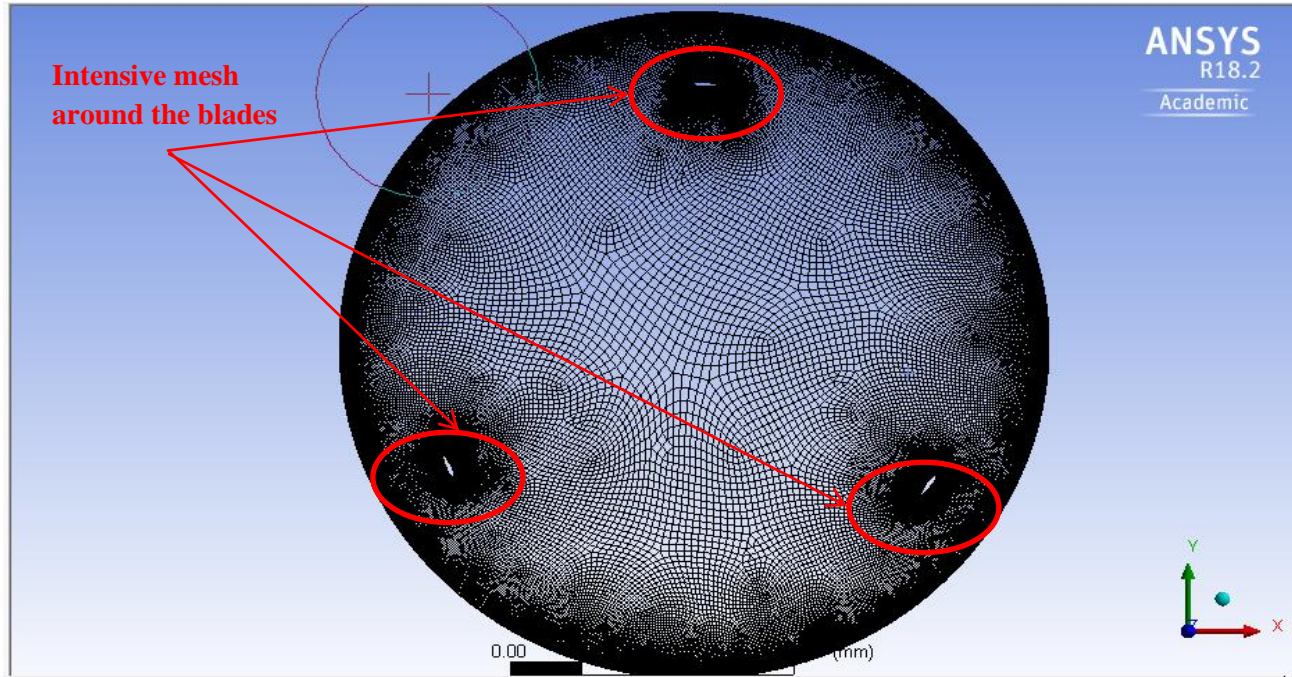


Figure III- 25: Rotating Domain Mesh Generation

The figure shows an intensive meshing around the airfoils due to the sensitivity of the Turbulence module to the meshing nodes and scale. As long as the scale smaller the simulation will be close to reality. Too many scenarios were simulated in order to minimize the number of nodes and enhance the quality of the meshing, whereas, **the above scenario was the best possible scenario.** As seen the below figure the Mesh Quality around the airfoils was good and hence minimize the computer time

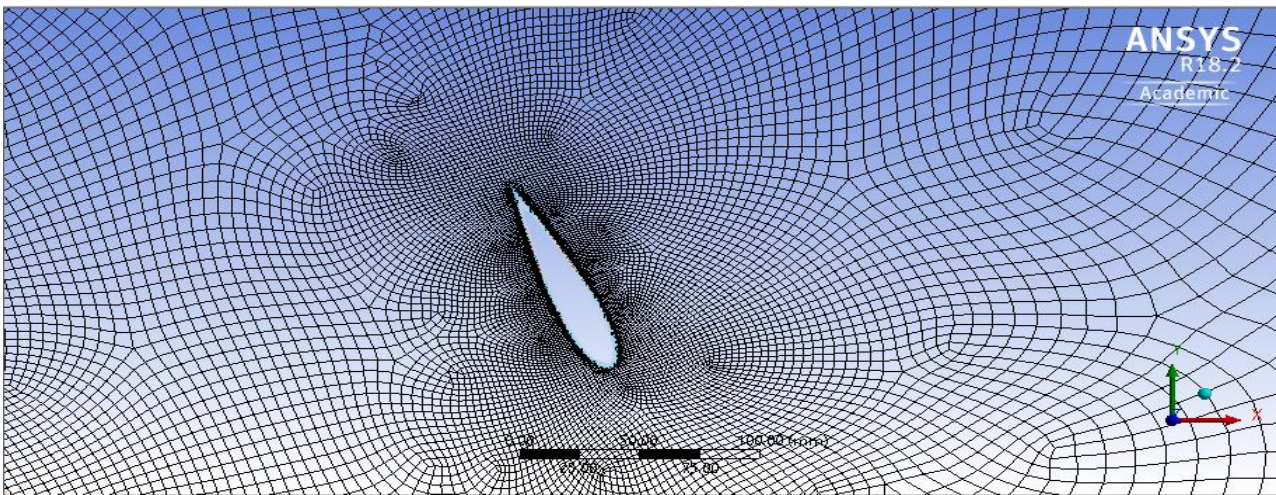


Figure III- 26: Mesh Around the Airfoils

After generating the mesh for two domains (Fixed and Rotating), Assembling figures 21 and 24 present the field of study as mention in the figure below

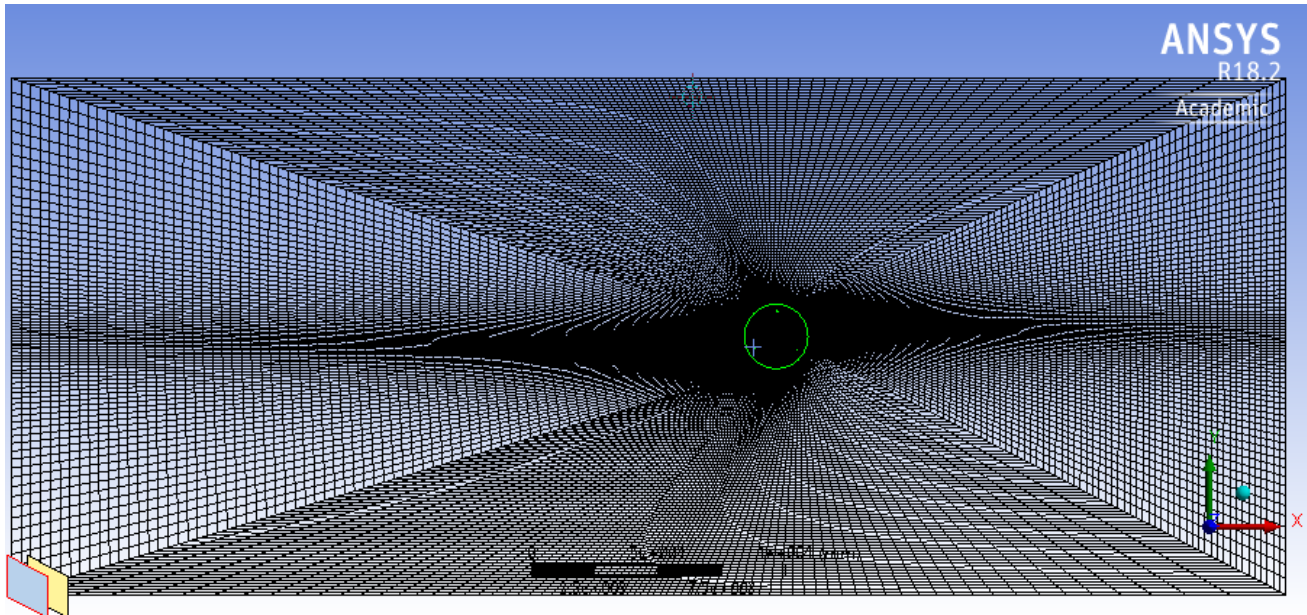


Figure III- 27:Rotating and Fixed Domain Mesh Generation

c- Mesh Quality Check (Skewness Factor)

Skewness is one of the primary quality measures for a mesh. Skewness determines how close to ideal (i.e., equilateral or equiangular) a face or cell, A skewness factor close to (0) means an **Excellent meshing** while skewness factor close(1) means **Poor Quality mesh**. Go to Mesh Detail\Display\change to Element Quality

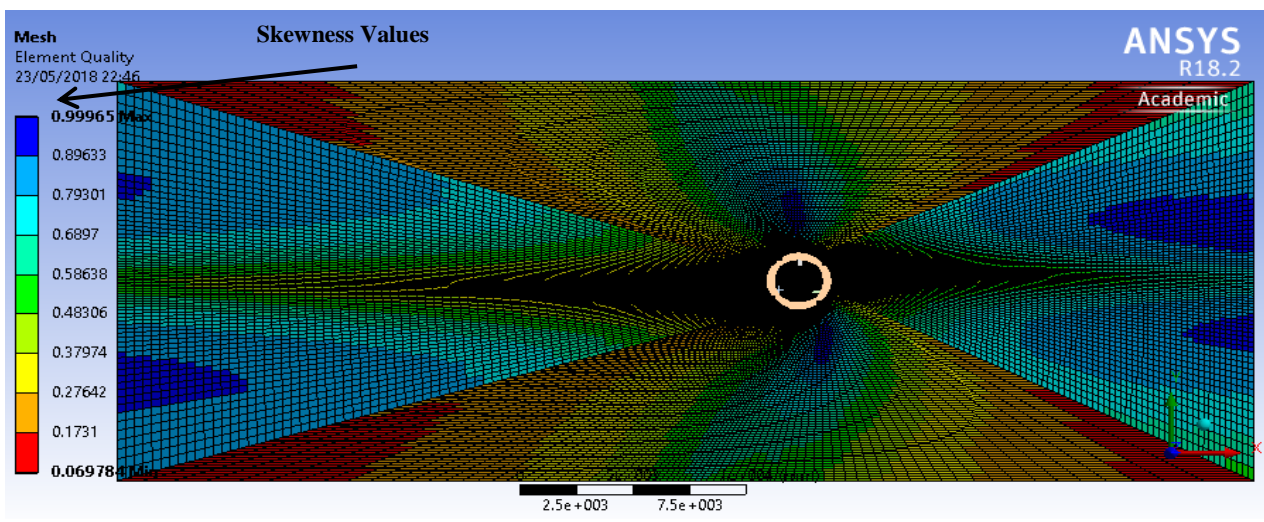


Figure III- 28: Skewness values for the generated Mesh

d- Name the Boundary Conditions**- Fixed Domain**

Go to select Edges/right click and select rename (Select Edge by Edge) as per below

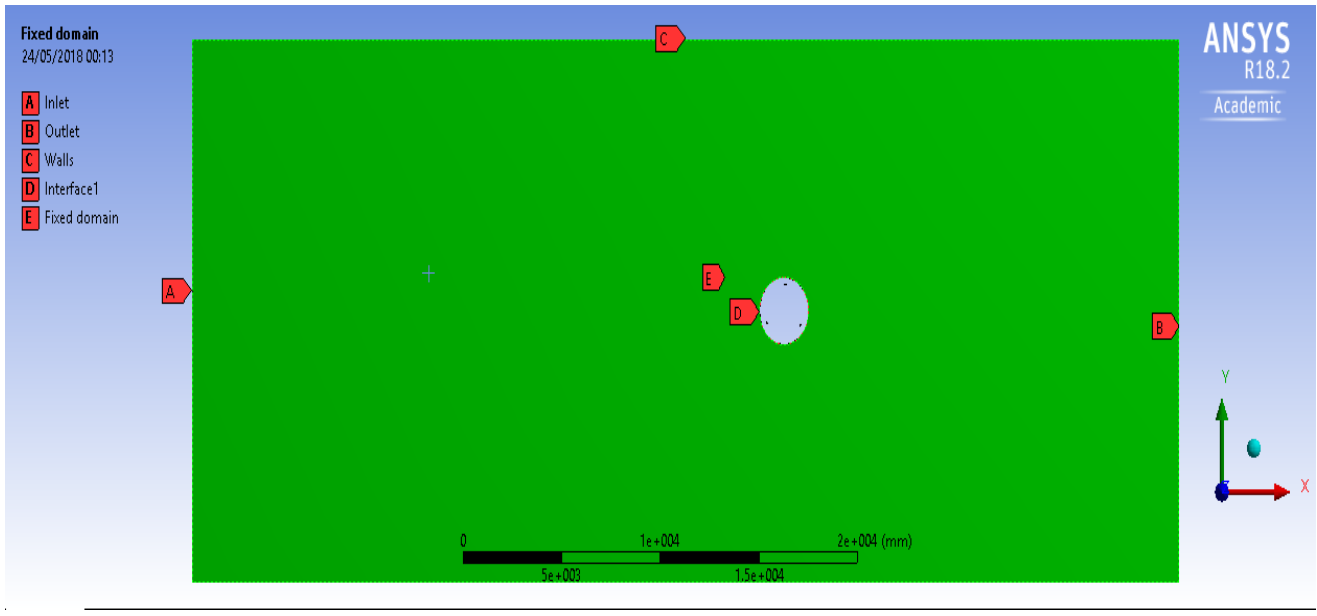


Figure III- 29:Fixed Domain Boundary Conditions

- Rotating Domain

Go to select Edges/right click and select rename (Select Edge by Edge) as per below

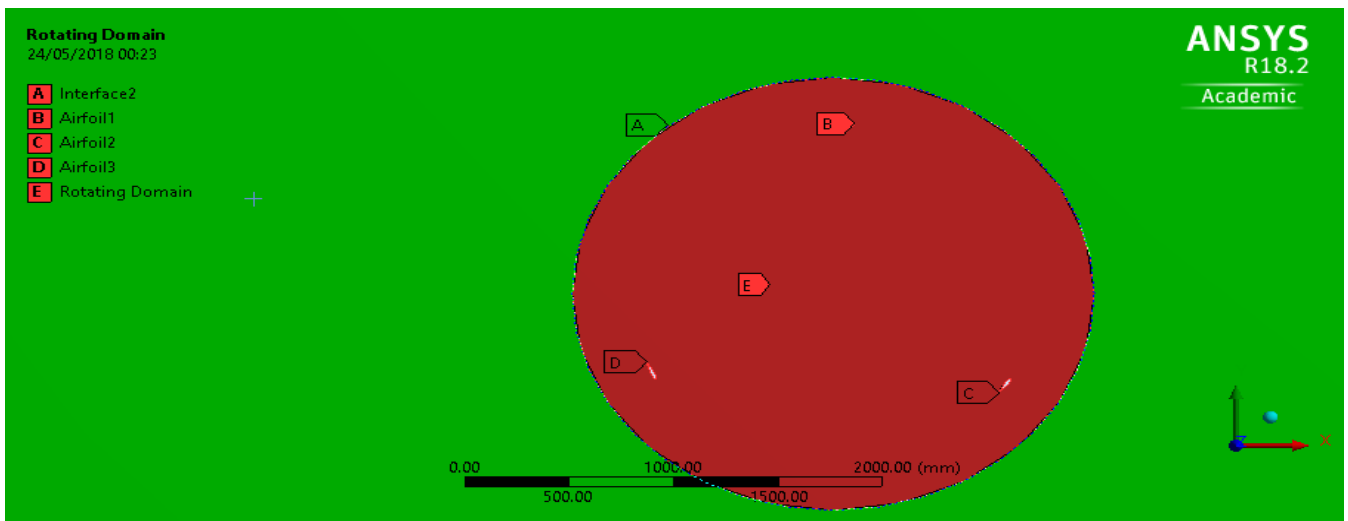


Figure III- 30:Rotating Domain Boundary Conditions

Once the boundary conditions being set, the meshing process is completed and ready to be exported to the solver **Fluent**. Go to File\Save Project then close Mesh Editor then Go to Setup double click the below windows will appear

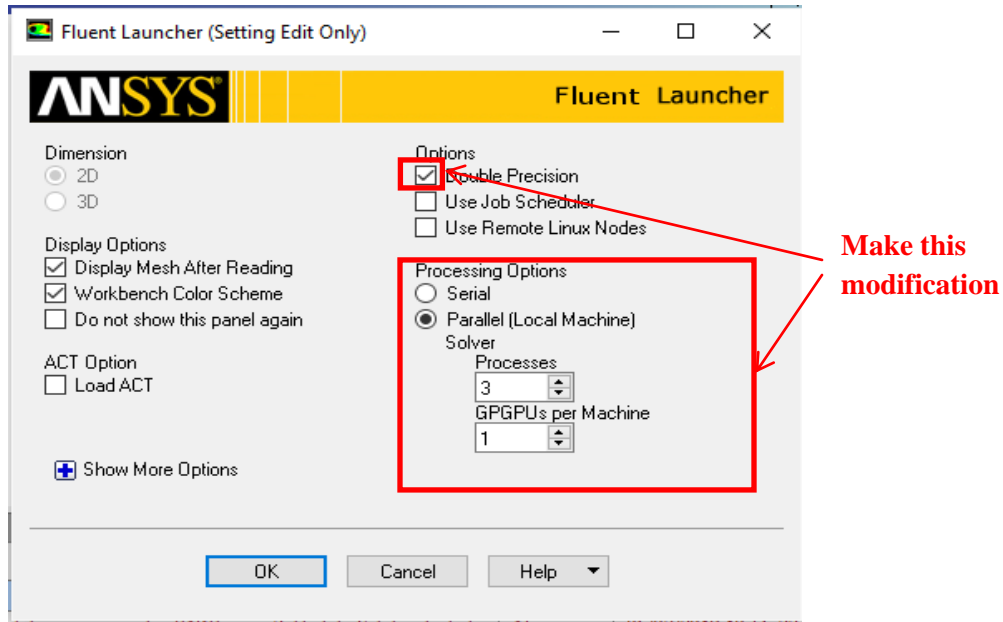


Figure III- 31:Fluent Launcher Setup

III.3.2.3 Solver Setup (4th Step)

III.3.2.3.1 General and Module

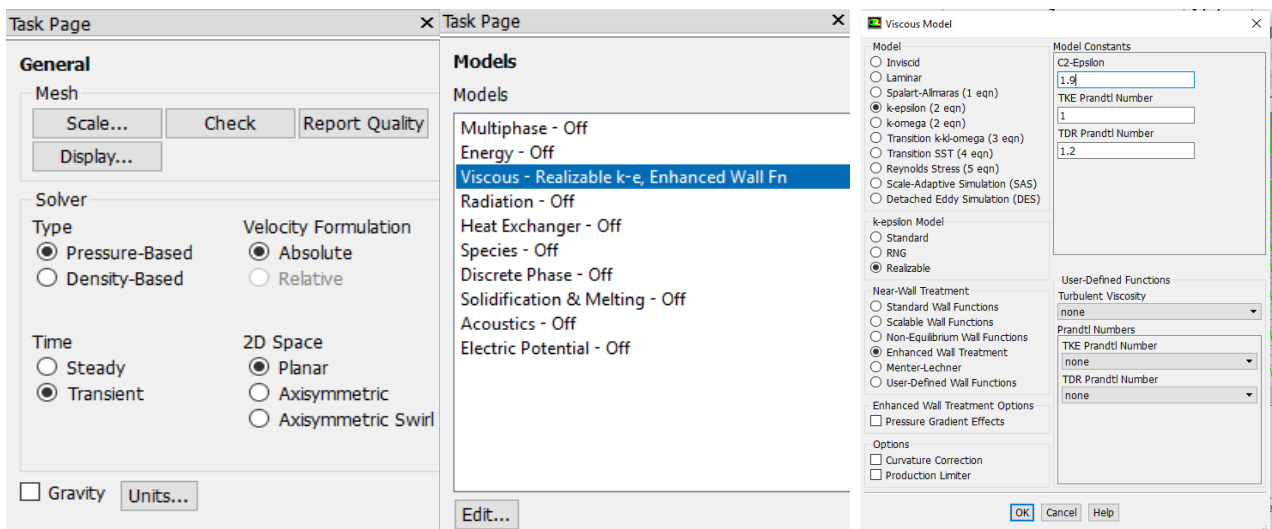


Figure III- 32:General and viscous Model setup

III.3.2.3.2 Materials

Choose Air as the material with the following parameters

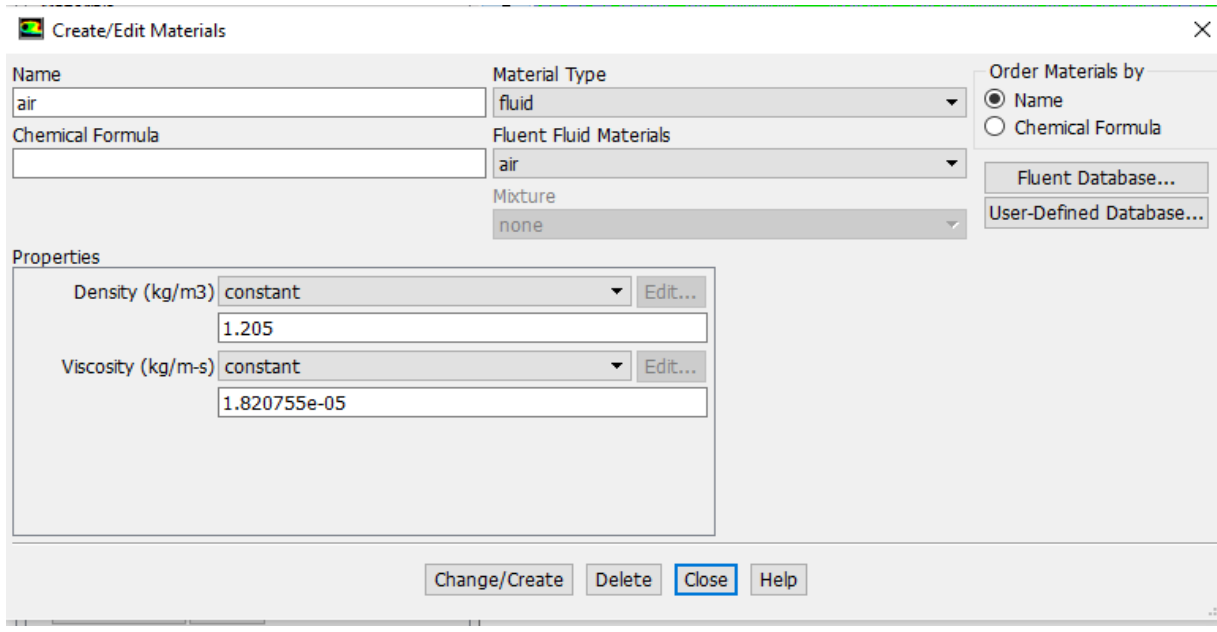


Figure III- 33:Material Editor Panel

III.3.2.3.3 Cell Zone Conditions

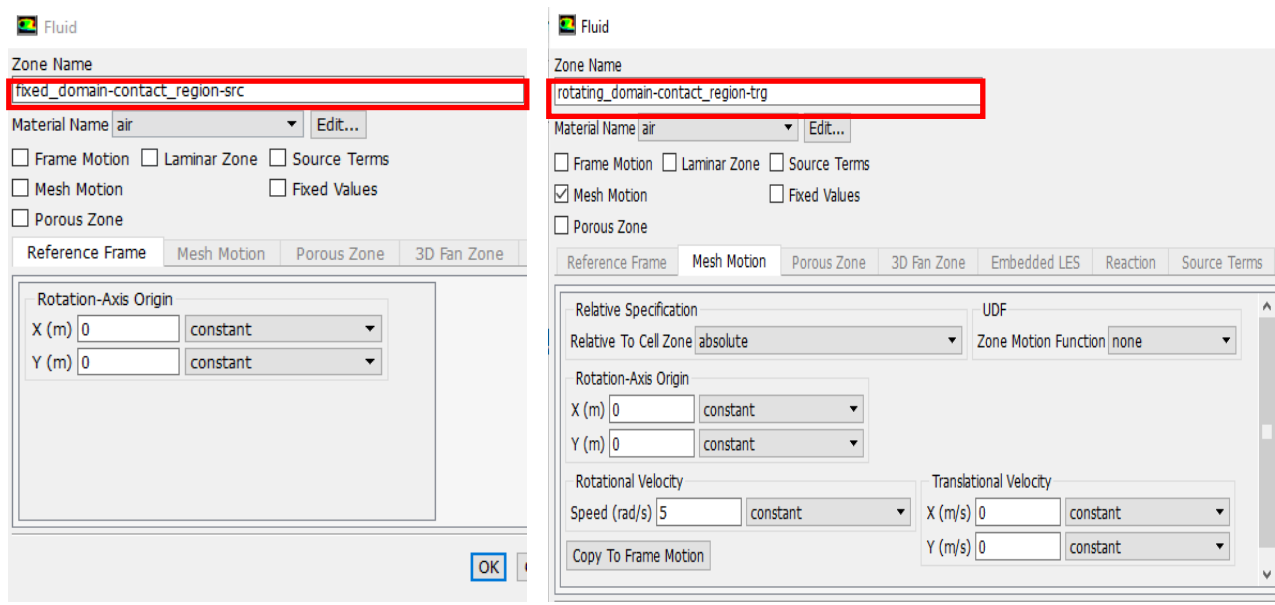


Figure III- 34:Cell Zone Conditions Setup

III.3.2.3.4 Boundary Conditions

Go to Inlet\double click. Input the following

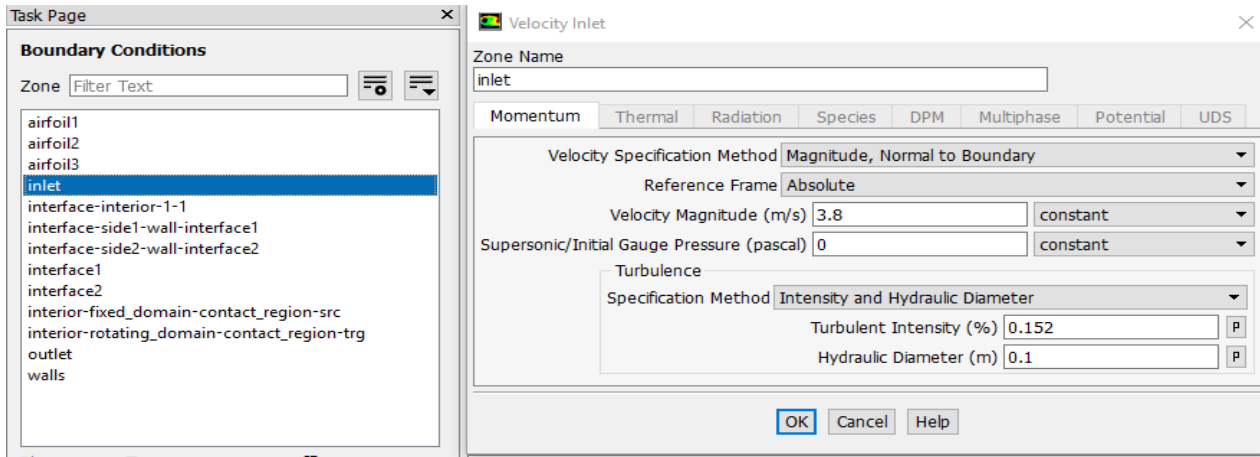


Figure III- 35:Inlet Setup

Table III- 5:Velocity Inlet input summary

Details	Input
Velocity Specification Method	Magnitude, Normal to Boundary
Reference Frame	Absolute
Velocity Magnitude (m/s)	3.8
Initial Gauge Pressure(Pa)	0
Turbulence Specification Method	Intensity and Hydraulic Diameter
Turbulent Intensity (%)	6
Hydraulic Diameter	1

Table III- 6:Pressure Outlet input summary

Details	Input
Backflow Reference Frame	Absolute
Gauge Pressure (Pa)	0
Pressure Profile Multiplier	1
Backflow Direction Specification Method	Normal to Boundary
Backflow Pressure Specification	Total Pressure
Turbulent Intensity (%)	6
Hydraulic Diameter	1

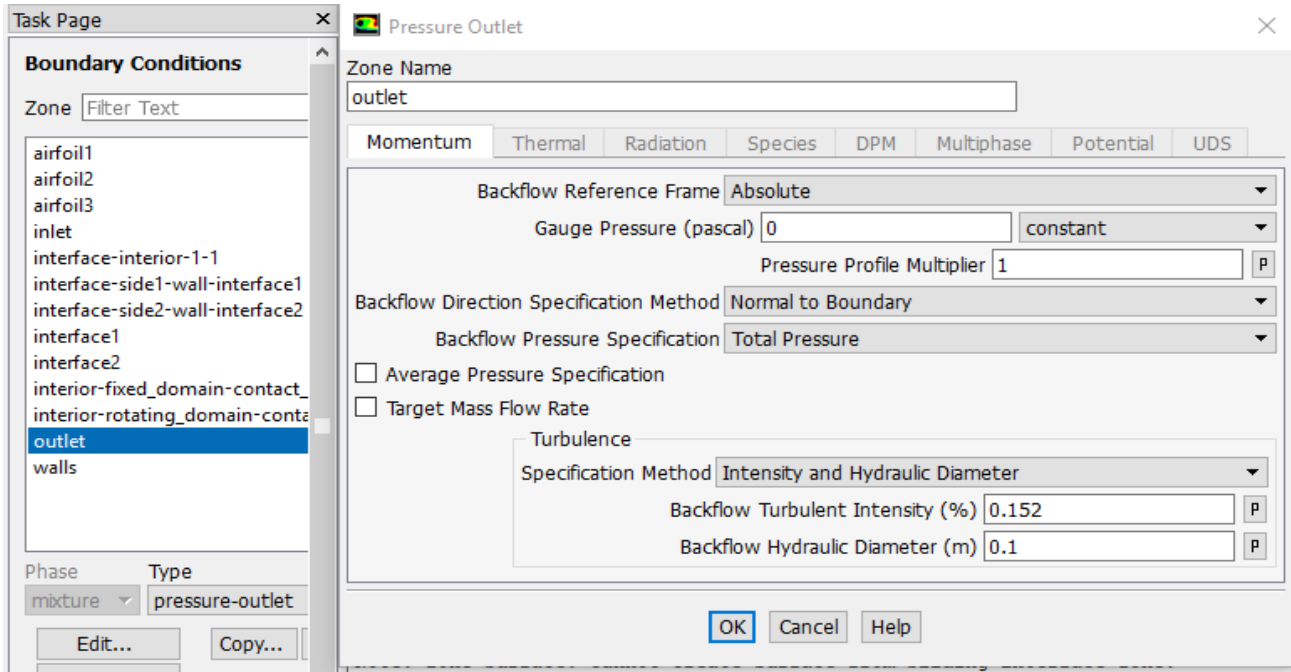


Figure III- 36:Outlet Setup

The Three Airfoils will be set to **stationary Wall with No slip for shear condition**, while in walls will be set to **Stationary Wall with Specified Shear for shear condition** as per the figure below

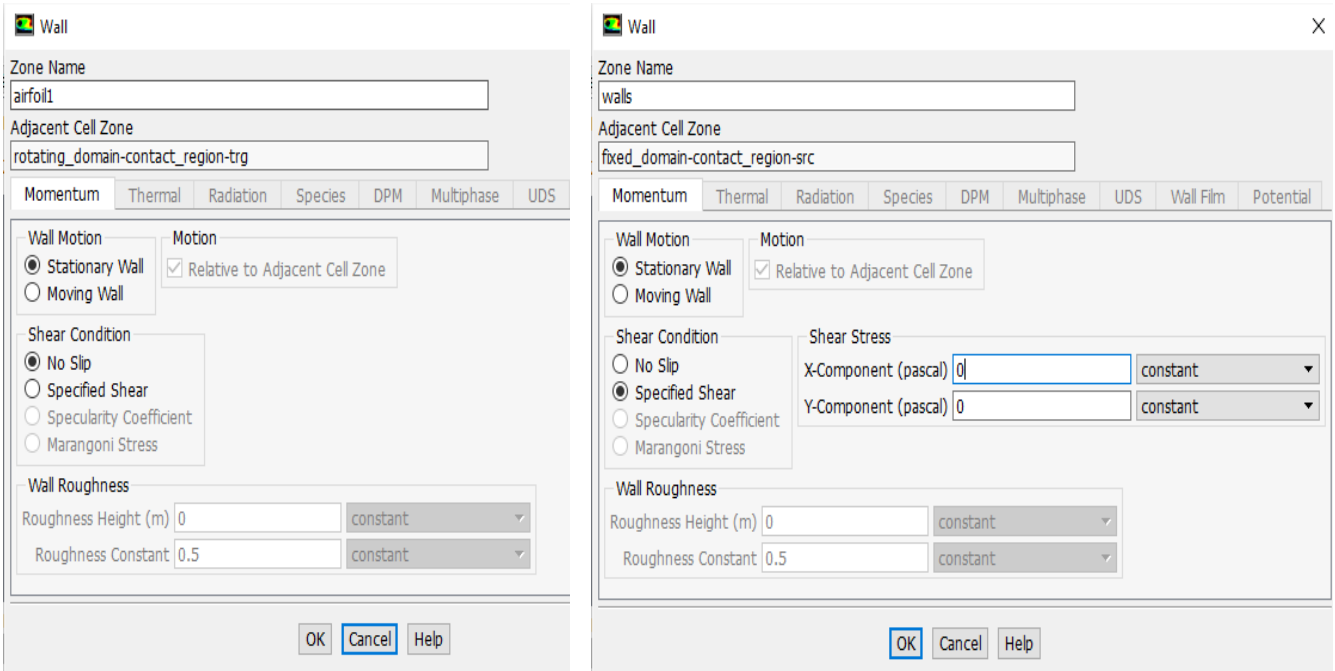


Figure III- 37:Airfoils and Walls Setup

III.3.2.3.5 Mesh Interface

Go to Mesh Interface\ Click Edit>Select Interface1 than Interface2\Click Create\Name it Interface

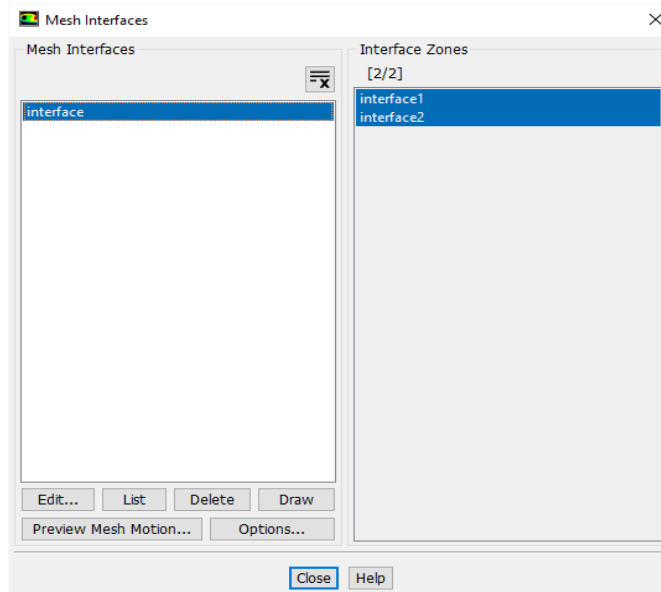


Figure III- 38:Mesh Interface Setup

III.3.2.3.6 Reference Values

Change Compute from to **Inlet** and Reference Zone to **Rotating Domain**, the Reference values automatically loaded

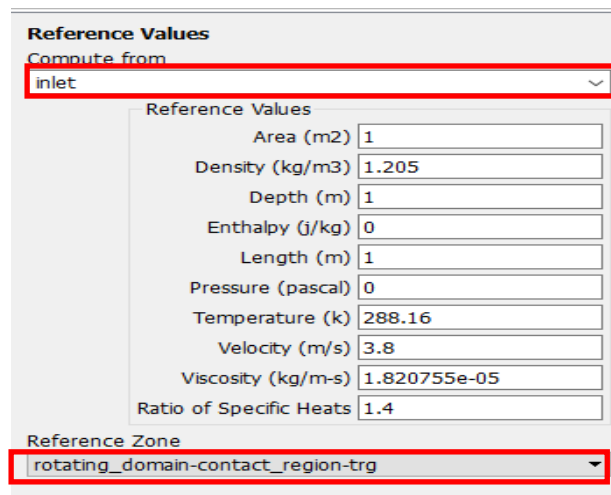


Figure III- 39:Reference Values Setup

III.3.2.4 Solution Setup (5^h Step)

III.3.2.4.1 Methods

Set the following input on Solution Methods, as per the table below

Table III- 7: Solution Methods input summary

Details	Input
Pressure –Velocity Coupling	
Scheme	SIMPLE
Spatial Discretization	
Gradient	Least Squares Cell Based
Pressure	Second Order
Momentum	Second Order Upwind
Turbulent Kinetic Energy	Second Order Upwind
Turbulent Dissipation Rate	Second Order Upwind
Transient Formulation	
Second Order Implicit	

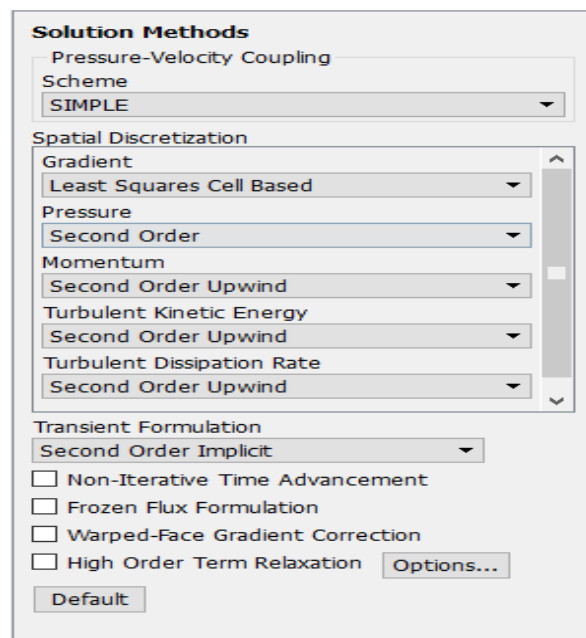


Figure III- 40: Solution Methods Setup

III.3.2.4.3 Controls

Set the following input on the Solution Controls, as per the table below

Table III- 8:Solution Controls input summary

Details	Input
Under-Relaxation Factors	
Pressure	0.3
Density	1
Body Forces	1
Momentum	0.7
Turbulent Kinetic Energy	0.8
Turbulent Dissipation Rate	0.8
Turbulent Viscosity	1

The screenshot shows the 'Solution Controls' dialog box with the 'Under-Relaxation Factors' section expanded. The following values are entered in the respective text boxes:

- Pressure: 0.3
- Density: 1
- Body Forces: 1
- Momentum: 0.7
- Turbulent Kinetic Energy: 0.8
- Turbulent Dissipation Rate: 0.8
- Turbulent Viscosity: 1

At the bottom of the dialog, there are buttons for 'Default', 'Equations...', 'Limits...', and 'Advanced...'.

Figure III- 41:Solution Controls Setup

III.3.2.4.3 Monitor

The following input must be implanted on Residual Monitors as per below figure

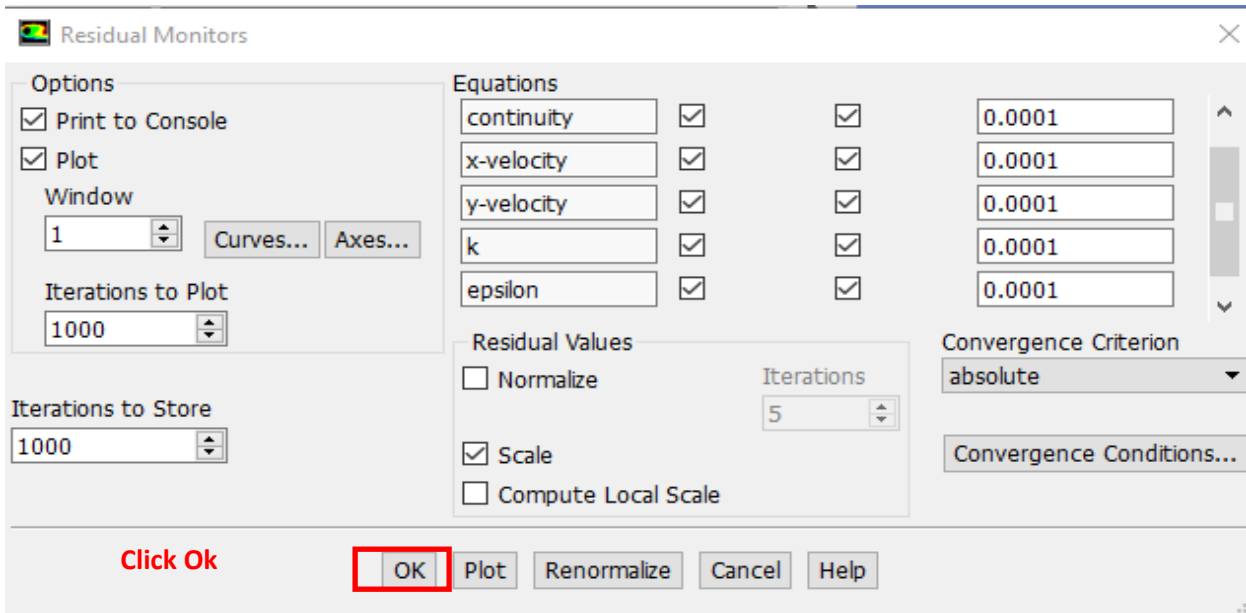


Figure III- 42:Residual Monitors Setup

III.3.2.4.4 Initialization

Choose **Standard Initialization** and choose **Inlet** for compute, the initial values automatically loaded than click **Initialize** as per below

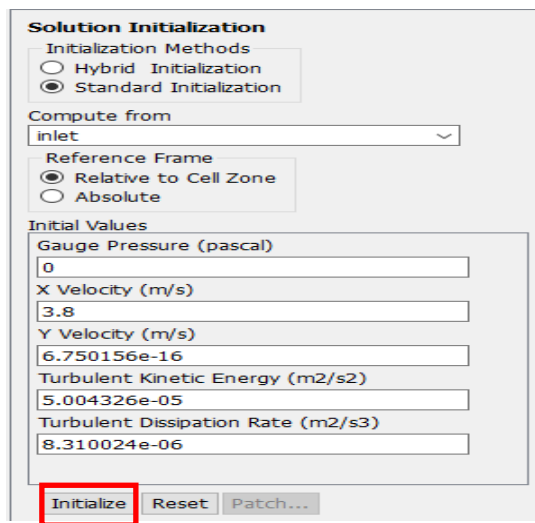


Figure III- 43: Initialization Setup

Once all the setup completed as described you should be able to check the case in Run Calculation, this step is very important in order to check if there is any error which not be accepted by the solver Fluent

III.3.2.4.5 Run Calculation

First once you click at **Check Case** you should be able to see (**No Recommendations to make at this time**), then click **Calculate**

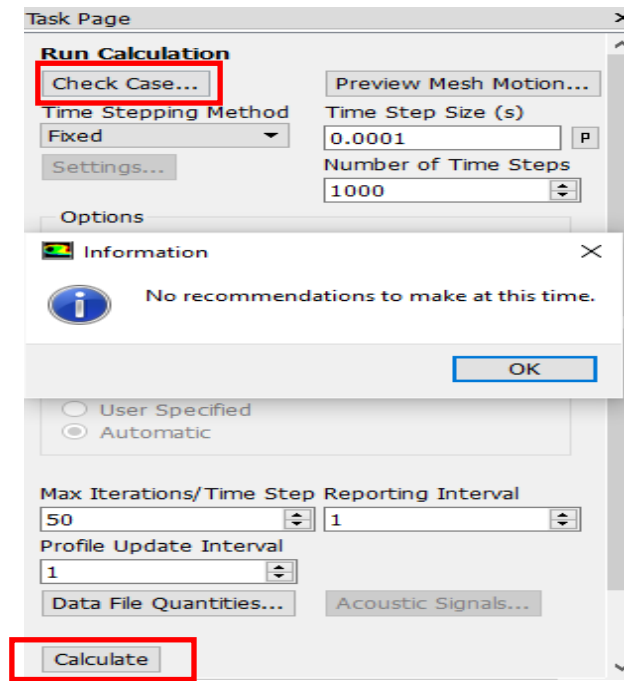


Figure III- 44:Run Calculation and check setup

III.4 Conclusion

Designing and optimizing workflow was an Excellent tool to best address the simulation challenges we face using a sliding mesh technic, Whoever, the setup of the ANSYS workbrench provide a vast knowledge of this simulation, therefore, the provides setup was implanted in order to confirm the suitable design for Ouargla wind speed of **3.8 m/s**.hence the computing time was a challenging factor due to the requirement of sliding mesh technic for the rotating and fixed domain.

Chapter IV
Simulation Results and
Discussion

Chapter IV

Simulation Results and Discussion

IV.1 Introduction

In this chapter i will discuss the results of the CFD simulation of my 2D designed H-Darrieus VAWT, Furthermore; we will be able to observe the Pressure, velocity and turbulence distribution inside the proposed wind tunnel. Furthermore we will observe the moment coefficient in order to calculate the power coefficient and validate the proposed 2D design.

IV.2 Pressure Contour

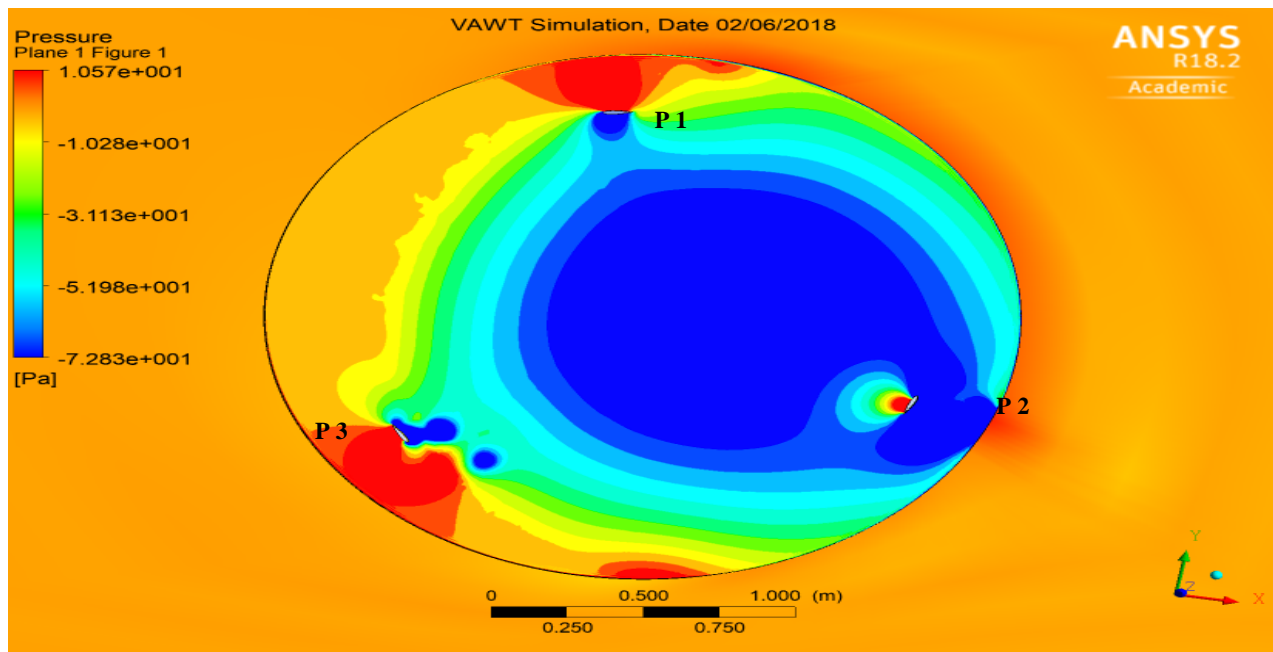


Figure IV- 1: Static Pressure Contour simulation results

The pressure acting on the airfoil results in a total pressure force. Splitting up this total pressure force into a part normal to the flow and another one tangential to the flow direction, results in a lift force and a drag force. In some regions, the pressure force acting on the extrados of the airfoil is higher as shown in red than the surrounding pressure while the intrados of the airfoils shows a low pressure. The following image shows the static pressure forces at 5.75 degangle of attack. The profile 3 and 1 contribute in the rotation of the wind turbine due the important difference in the static pressure between the extrados and intrados whereas the lift force is important.

Moreover, the pressure is high on the concave side of the rotor blade P1 and P2 as that is where the wind will hit the most and will not escape as fast as on the convex side. Negative pressure (vacuum gauge pressure – relative to the atmospheric pressure) is generated on the backside of the rotor, which makes sense as this a static case where the rotor is fixed in this specific orientation. This pressure differential causes a net force on the blades and hence causes rotation.

IV.3 Velocity Contour

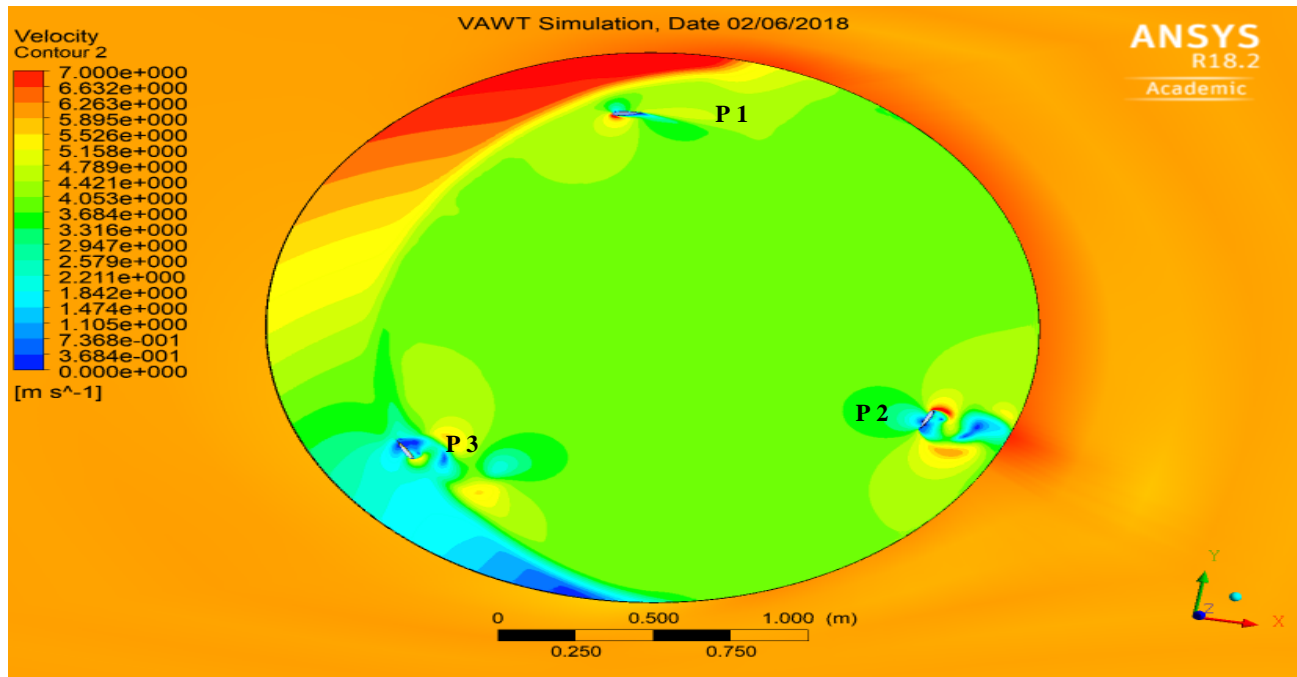


Figure IV- 2: Velocity Contour simulation results

Figure IV-2 shows a distribution of the wind velocity at the rotating domain of the designed wind turbine, whereas, the velocity decreased on the extrados and intrados of the following profiles (P3 et P2) due to observed high static pressure as seen in figure IV-1, Velocity and pressure are dependent on each other - Bernoulli's equation says that increasing the velocity decreases the local pressure and vice versa, however, the velocity at the extrem left of the leading edge of the profile 1 and 2 seems to be lightery higher.

IV.4 Turbulence Kinetic Energy Contour

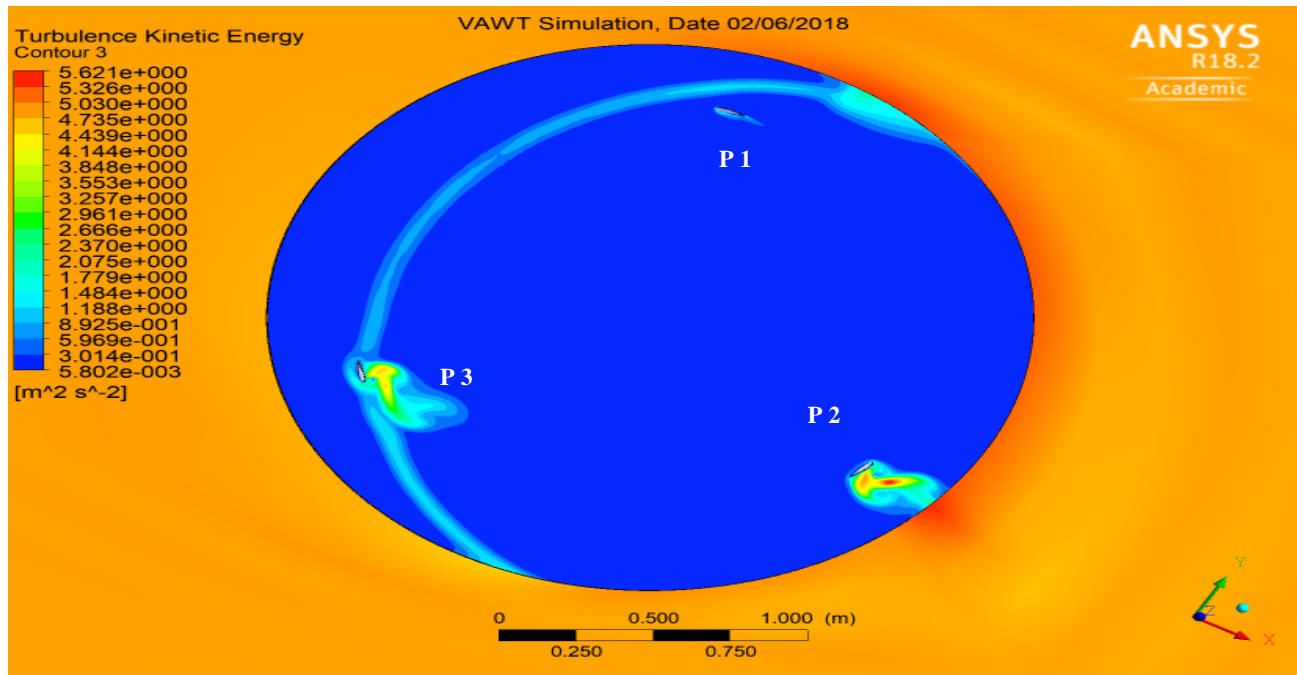


Figure IV- 3: Turbulence kinetic energy Contour simulation results

Figure IV-3 shows the turbulent kinetic energy distribution at the rotating part of the H-Darrieus wind turbine, the profile 2 and 3 generate more turbulence due to the interaction of these profiles with the streamlines of the incompressible fluid in movement.

This turbulence is created in the inverse direction of the flow as seen on the intrados of profile 3 and extrados of profile 2. Profile 1 is not contributing to the turbulence at this position due to non-intersection with the wind streamlines.

IV.5 Velocity Vector

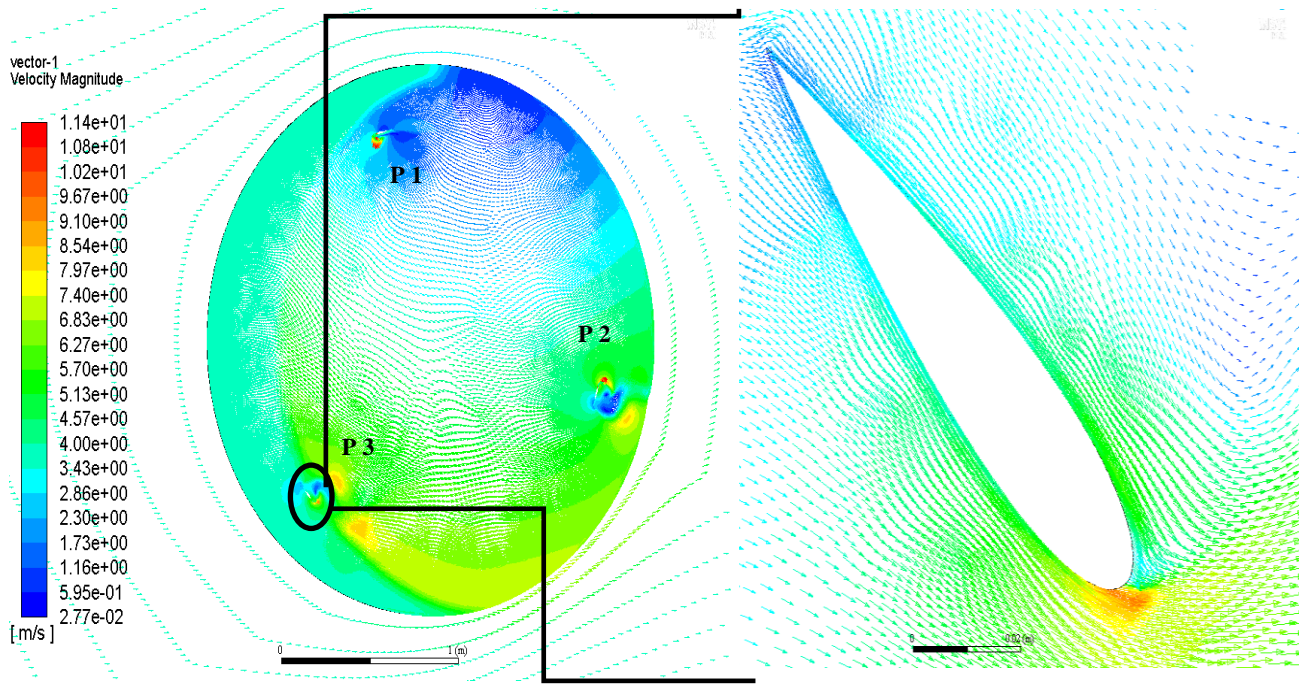


Figure IV- 4: Velocity vector Distribution

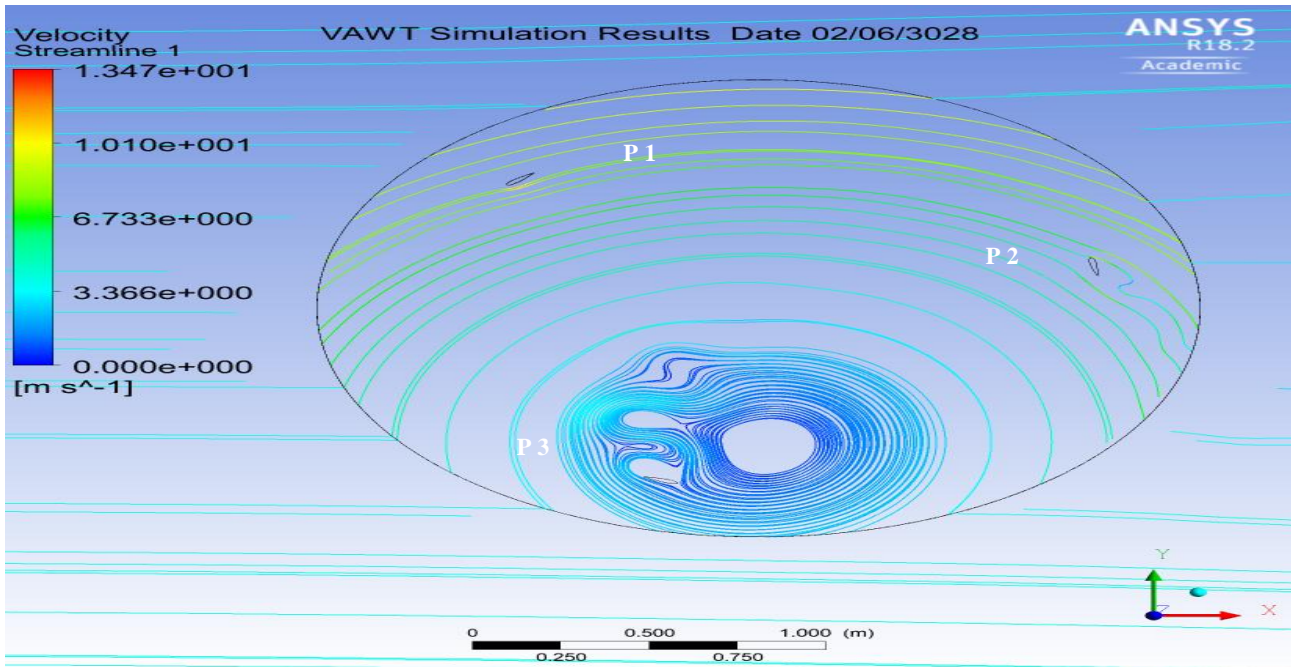


Figure IV- 5: Velocity streamline

As seen the Figure IV-6 the wake created by the profile number 3 at low angular rotation created by the low velocity turbulence the flow field is fairly uniform and the wake of the advancing blade 1 can be seen to influence the flow near the following blade especially the blade number 3. As the rotor turns the flow field begins to “polarize” into two diametrically opposed regions. A high speed region enveloping the single advancing blade – which does no longer “feel” the wake of the previous blade 3 and a low speed region delimited by the other two blades (which are, largely, in symmetrical positions). This behavior later reduces as the rotor turns and the flow field tends to become uniform. It is interesting to observe that, in this case, the mere fact that the top blade loses the downwash wake of the previous blade leads to a slight acceleration of the fluid in its region. However, this acceleration works “against” the turning of the rotor.

IV.6 Pressure Vector

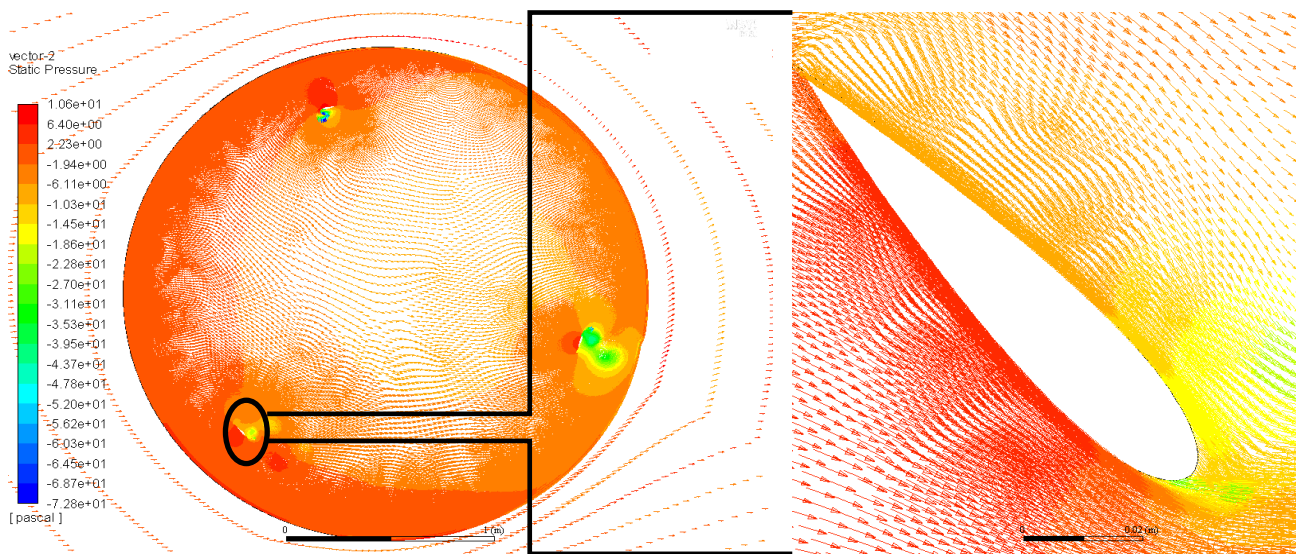


Figure IV- 6:Pressure vector Distribution

IV.7 Validating the design

Validation of the 2D design by the performance coefficient, C_p depends on the type of airfoils, blade thickness and Reynolds number. It is basically given by the ratio between power extracted by the turbine and available wind power. It can be mathematically expressed as:

$$C_p = \lambda_{opt} \times T_{mean} \quad \text{(IV-1)}$$

Where

λ_{opt} : The optimum tip speed ratio Equal to 6 for VAWT.

T_{mean} : is the average torque reported by coefficient of moment in FLUENT for one complete revolution. The reported moment coefficient C_m for our simulation is **0.0831** presented in the below figure IV-7

Moments - Moment Center (1 0 0) Moment Axis (0 0 1)						
Zone	Moments (n-m)			Coefficients		
	Pressure	Viscous	Total	Pressure	Viscous	Total
airfoil2	0.72192727	0.0010941342	0.7230214	0.082979192	0.0001257611	0.083104953
Net	0.72192727	0.0010941342	0.7230214	0.082979192	0.0001257611	0.083104953

Figure IV- 7: Reported Moment Coefficient by FLUENT

Therefore,

$$C_p = \lambda_{opt} \times T_{mean} = \lambda_{opt} \times C_m = 6 \times 0.08310 = 0.4986$$

Some studies explain that the 2D simulation present an overestimation of 6-8% comparing to 3D, hence, the above power coefficient will be reduced by 8% to match the reality, therefore, Our reported power coefficient $C_p = 0.45$ which explain that our design is the best optimized 2D VAWT.

IV.8 Conclusion

The results of the simulation presented above shows the complexity of the velocity, pressure and turbulence field, where the lift and drag coefficient for the airfoils NACA0018 play an importance rules in generating a rotating movement at speed of 3.8 m/s.

In this simulation we were able to see that blades number 3 and 2 are contributing most on the rotation of the our wind turbine, Furthermore, the simulation moment coefficient reported on the FLUENT shows an optimum power coefficient of 0.45 which validate the proposed 2D design, the 2D simulation provide a good understanding on the forces and pressure our H-Darrieus VAWT, hence the 3D simulation provides an Excellence close to reality, this simulations relay on the viscous model chosen to best approach the real case, however, a real tunnel test is required in order to validate the design of the turbine.

Conclusion and Recommendations

In the present work an unsteady 2D CFD model of H-Darrieus VAWT was developed to evaluate rotor performance and support rotor design and wind tunnel experiments. Computational domain, mesh, solver settings and Transition turbulence model local correlation parameters were optimized. To take into account the unsteady rotational effects, a Sliding Mesh Model was used optimizing the time step of the transient solver. Grid and time step independent solutions were reached after a long process of refinement.

In this project I went through the solid workflow in order to optimize the turbine dimension, furthermore, the low region wind speed was a challenging factor to best design our rotor, however, the turbine simulations were performed using a both turbulent k- ϵ realizable model with Enhanced wall treatment and K- ω to demonstrate the superior predictive capabilities of the modified Transition model.

At this project ANSYS 18.2 was used as a complete set of multiphysic software that best simulate the CFD simulation through a Fluent solver. The simulation shows a slight overestimation for the Transition model and this is due to the limits of a 2D modelization that does not take into account 3D effects (i.e. tip vortex). For this reason the authors will use this methodology to develop a 3D CFD model in the future research and assesses whether improvements justify the great increase of calculation time. However, considering the good predictive results of the 2D CFD model, this will be used in the future to support experiments in the proprietary, furthermore, a tunnel test it's a most to best evaluate the simulation results which need to be considered in the next project.

Due to the proposed field of study that represent the tunnel test(50X20m) the number of nodes and elements were bigger, hence, the calculation time was too long for my machine, therefore, it was decided to reduce the field of study to its least allowed surface for this type of wind turbine.

Recommendations for the Future Work

- 3-D model of a VAWT can be proposed in the future studies to account for the tip vortices and rotor arms. The 2-D CFD simulation does not include the effects of the end tip vortices present on the real wind turbine and that is why, 2D simulations shows a significantly increased performance compared to the 3D simulations. Furthermore, the other reason for an

Conclusion and Recommendations

overestimated numerical value of C_p of 2-D calculations as compared to 3-D could be the absence of rotor arms in 2-D simulations.

- In lieu of having a blade fixed to the rotor arm, a flapping or plunging mechanism can be provided which will help reducing the condition of a dynamic stall. It is the same phenomena used by insects.

References

- [1] Eddahmani Aymane. Savonius Vertical Wind Turbine - Design Simulation and Physical Testing (May 2017).
- [2] M.H. Mohamed. CFD analysis for H-rotor Darrieus turbine as a low speed wind energy converter (2015).
- [3] Farouk Chellali. A contribution in the actualization of wind map of Algeria(2011).
- [4] Ferziger Peric. Computational Methods for Fluid Dynamics (3rd Ed – 2002).
- [5] Ion Malaeli. Numerical Simulation of VAWT Flow using Fluent* (2014).
- [6] FadyJamati. Étude Numérique D'une Eolienne Hybride Asynchrone (2011).
- [7] Dimitrios Sofialidis. Using Moving Reference Frames and Sliding Meshes workshop (2013).
- [8] Saqib Hameed. Evaluation of Aerodynamic Forces over a Vertical Axis Wind Turbine Blade through CFD analysis (2007).
- [9] Kadri Mohamed Ayoub. Etude de l'écoulement d'air à travers une Eolienne Darrieus de type H à pale NACA4412 (2015).
- [10] Naimi Abdelmalek. Etude et simulation numérique d'une Eolienne hybride Savonius-Darrieus.
- [11] ANSYS help.

Internet Web Sites

- [12] <https://www.cfd-online.com/Forums/>
- [13] <http://airfoiltools.com/NACA0018>
- [14] <https://www.ansys.com/services/training-center>

Annex

Annex

What is CFD?

Flows and related phenomena can be described by partial differential (or integro-differential) equations, which cannot be solved analytically except in special cases. To obtain an approximate solution numerically, we have to use a discretization method which approximates the

Differential equations by a system of algebraic equations, which can then be solved on a computer. The approximations are applied to small domains in space and/or time so the numerical solution provides results at discrete locations in space and time. Much as the accuracy of experimental data depends on the quality of the tools used, the accuracy of numerical solutions is dependent on the quality of **discretization** used. Contained within the broad field of computational fluid dynamics are

activities that cover the range from the automation of well-established engineering design methods to the use of detailed solutions of the **Navier-Stokes equations** as substitutes for experimental research into the nature of complex flows. At one end, one can purchase design packages for pipe systems that

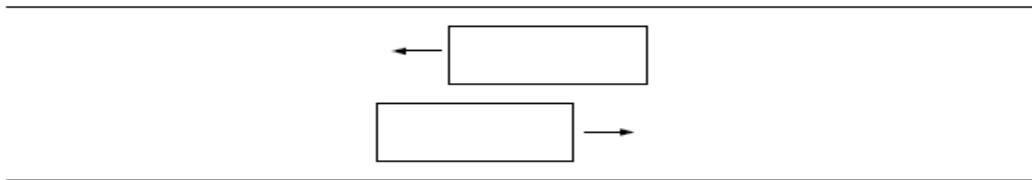
solve problems in a few seconds or minutes on personal computers or workstations. On the other, there are codes that may require hundreds of hours on the largest super-computers. The range is as large as the field of fluid mechanics itself, making it impossible to cover all of CFD in a single work.

Also, the field is evolving so rapidly that we run the risk of becoming out of date in a short time. We shall not deal with automated simple methods in this book. The basis for them is covered in elementary textbooks and undergraduate courses and the available program packages are relatively easy to understand and to use. We shall be concerned with methods designed to solve the equations of fluid motion in two or three dimensions. These are the methods used in nonstandard applications, by which we mean applications for which solutions (or, at least, good approximations) cannot be found in textbooks or handbooks. While these methods have been used in high-technology engineering (for example, aeronautics and astronautics) from the very beginning, they are being used more frequently in fields of engineering where the geometry is complicated or some important feature (such as the prediction of the concentration of a pollutant) cannot be dealt with by standard methods. CFD is finding its way into process, chemical, civil,

and environmental engineering. Optimization in these areas can produce large savings in equipment and energy costs and in reduction of environmental pollution.

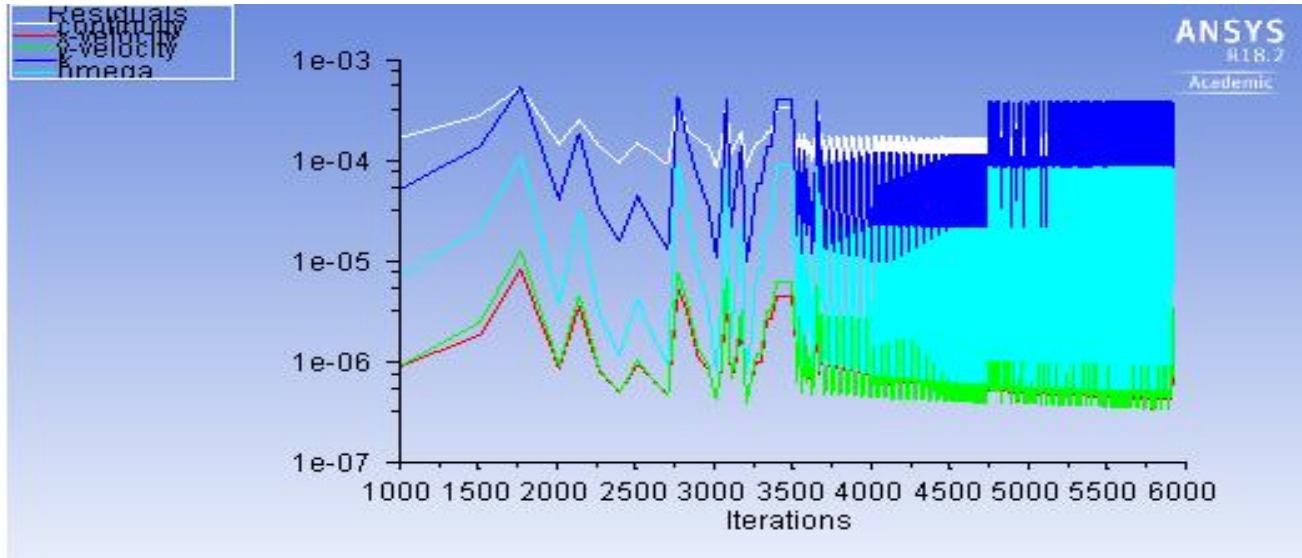
Sliding Meshes?

When a time-accurate solution for rotor-stator interaction (rather than a time-averaged solution) is desired, you must use the sliding mesh model to compute the unsteady flow field. As mentioned in Section 9.1, the sliding mesh model is the most accurate method for simulating flows in multiple moving reference frames, but also the most computationally demanding.



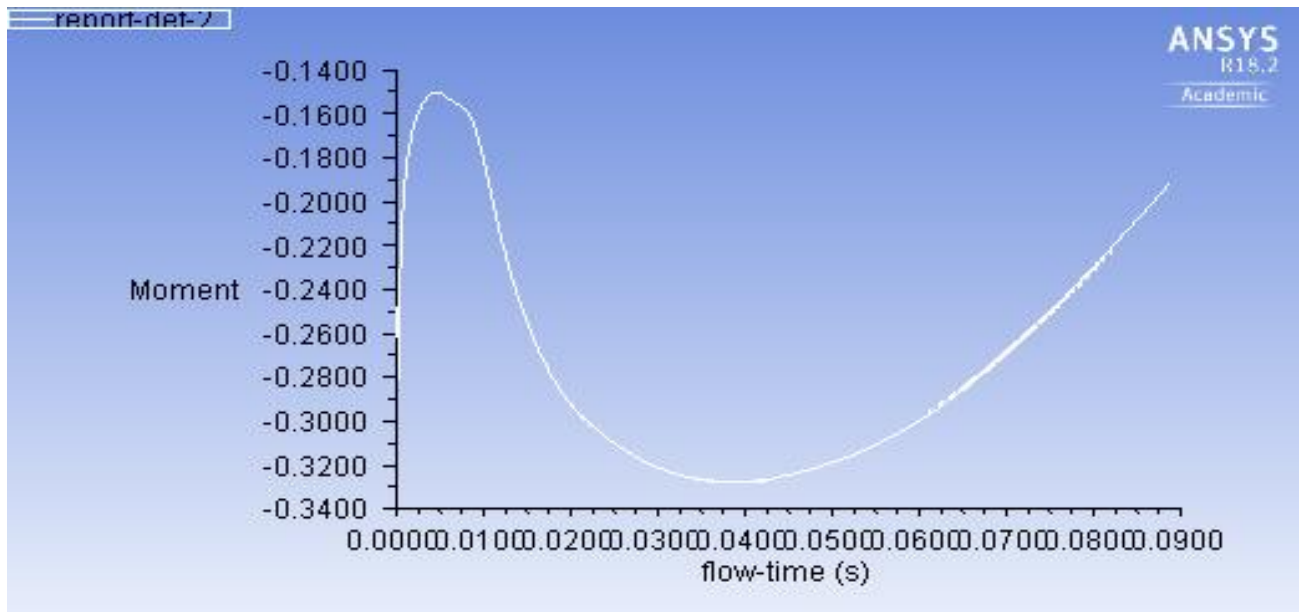
Most often, the unsteady solution that is sought in a sliding mesh simulation is time-periodic. That is, the unsteady solution repeats with a period related to the speeds of the moving domains. However, you can model other types of transients, including translating sliding mesh zones (e.g., two cars or trains passing in a tunnel, as shown in Figure 9.5.1). Figure 9.5.1: Two Passing Trains in a Tunnel Note that for flow situations where there is no interaction between stationary and moving parts (i.e., when there is only a rotor), the computational domain can be made stationary by using a rotating reference frame. (See Section 9.2 for details.) When transient rotor-stator interaction is desired, you must use sliding meshes. If you are interested in a steady approximation of the interaction, you may use the multiple reference frame model or the mixing plane model.

Simulation Residual Plot



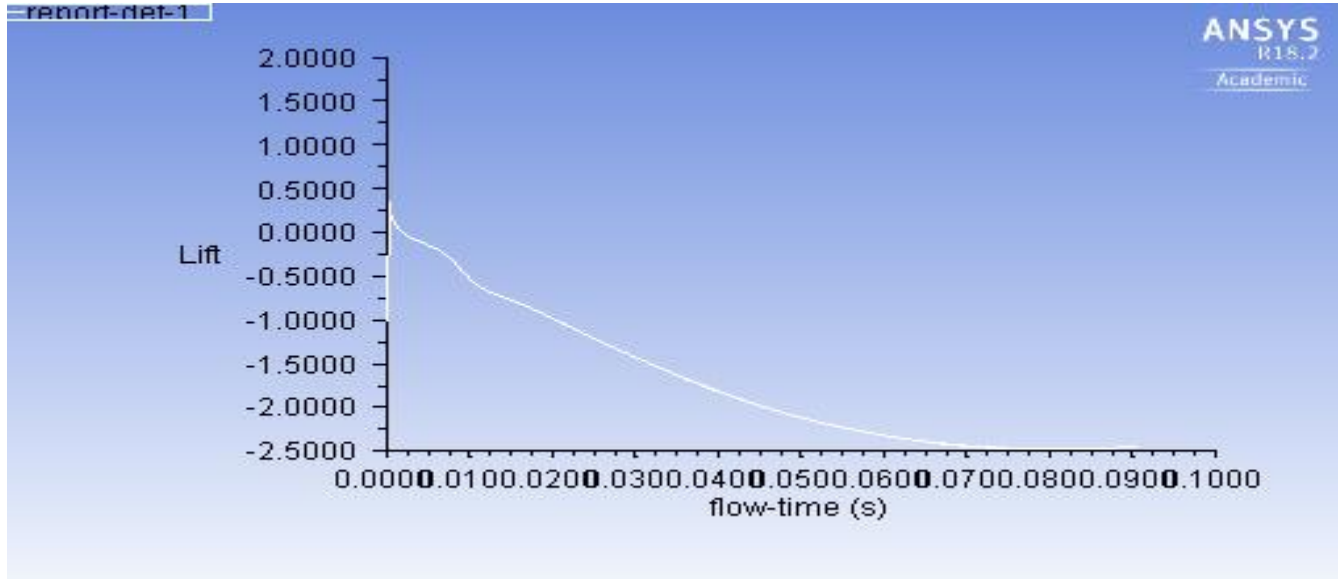
Simulation Residual Plot

Moment Coefficient



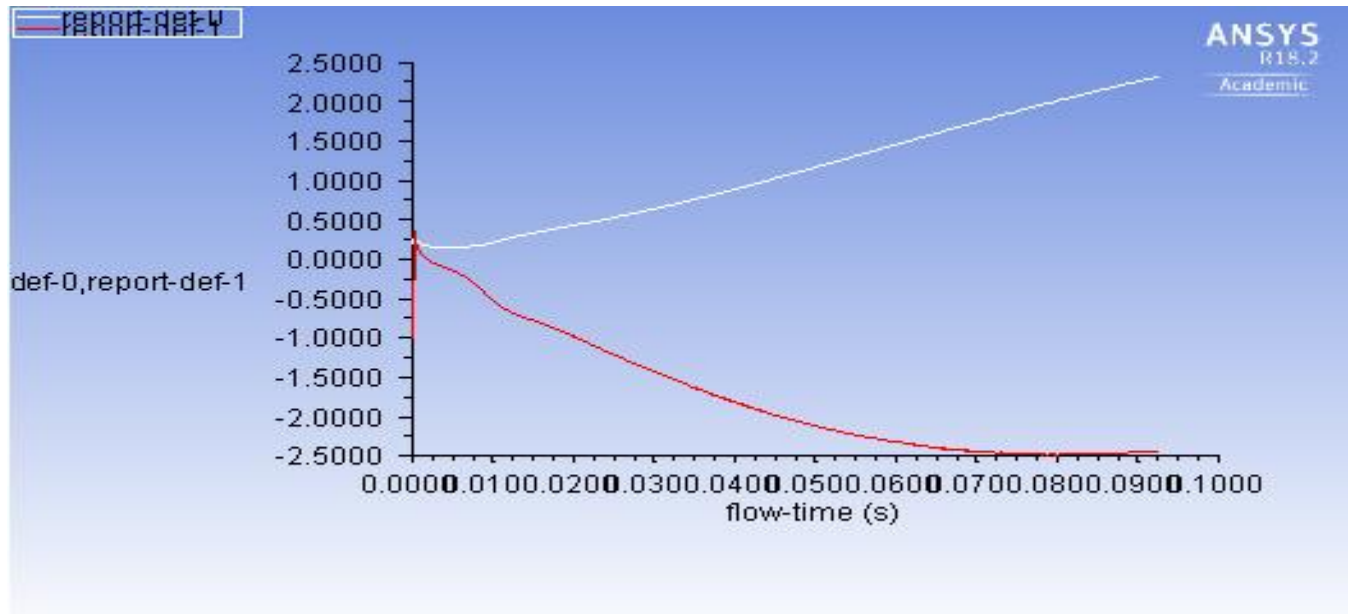
Simulation Moment Coefficient

Lift Coefficient



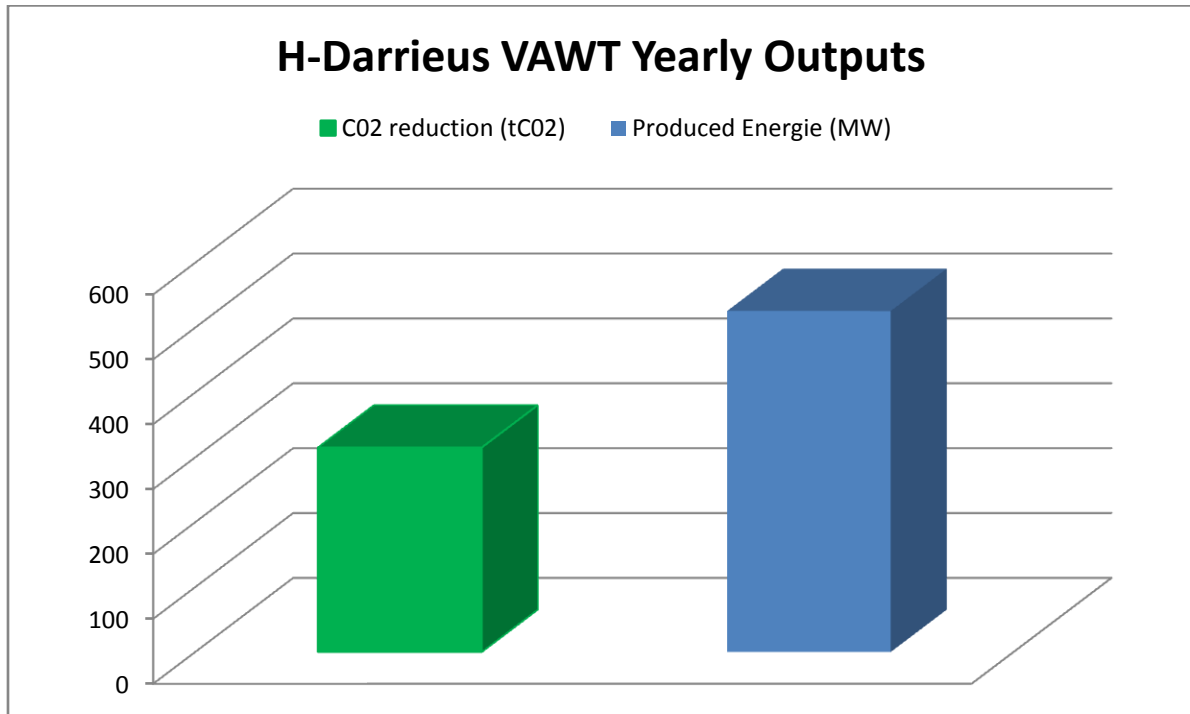
Simulation Lift Coefficient

Drag and Lift Coefficients

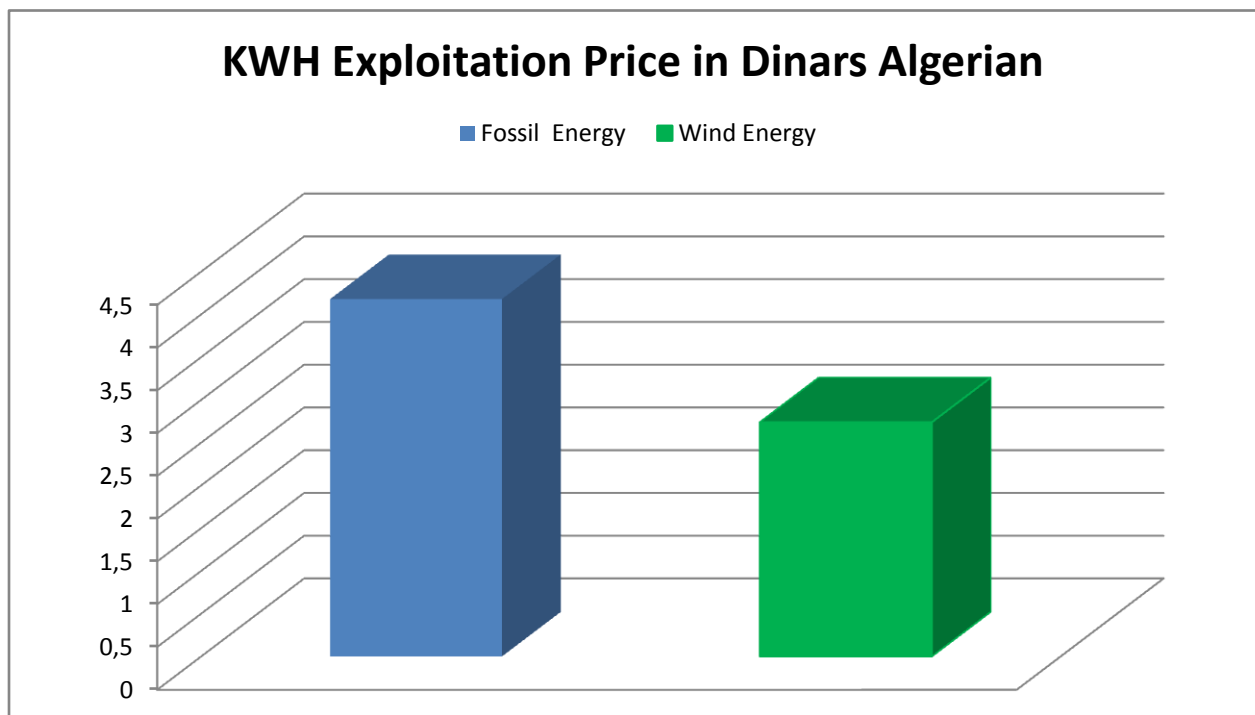


Simulation Drag and Lift Coefficients

C02 footprint



KWH Price in Algeria



NACA0018 Profile Data

X	Y	Z
0,00000	0,00000	0
0,01250	0,02841	0
0,02500	0,03922	0
0,05000	0,05320	0
0,07500	0,06300	0
0,10000	0,07024	0
0,15000	0,08018	0
0,20000	0,08606	0
0,25000	0,08912	0
0,30000	0,09003	0
0,40000	0,08705	0
0,50000	0,07941	0
0,60000	0,06845	0
0,70000	0,05496	0
0,80000	0,03935	0
0,90000	0,02172	0
0,95000	0,01210	0
1,00000	0,00189	0
0,00000	0,00000	0
0,01250	-0,02841	0
0,02500	-0,03922	0
0,05000	-0,05320	0
0,07500	-0,06300	0
0,10000	-0,07024	0
0,15000	-0,08018	0
0,20000	-0,08606	0
0,25000	-0,08912	0
0,30000	-0,09003	0
0,40000	-0,08705	0
0,50000	-0,07941	0
0,60000	-0,06845	0
0,70000	-0,05496	0
0,80000	-0,03935	0
0,90000	-0,02172	0
0,95000	-0,01210	0
1,00000	-0,00189	0

Abstract

In this memory, 2D dimensional unsteady flow around an H-Darrieus vertical axis winds turbine (VAWT) comprising three rotating symmetric airfoils (NACA0018) was studied numerically with the consideration of the near wake. The flow around the wind turbine was simulated using ANSYS 18.2. A workflow of the design was used to optimize the performance of the rotor then, a CFD was used to generate grid for the designed rotor a sliding mesh technique was generated to create a moving mesh. Realizable k- ϵ turbulence model was employed for the analysis and simulation was set at the region wind speed of 3.8 m/s. Due to lack of tunnel test the simulation results was used as reference in order to validate the design.

Key words: H-Darrieus VAWT, Sliding Mesh Technique, ANSYS®, Unsteady Flow, NACA0018

المخلص

في هذه الاطروحة تمت دراسة التدفق الثنائي الابعاد غير المستقر حول التوربين عمودي المحور اللذي يتألف من ثلاثة اجنحة متناظرة دوارة من نوع (NACA 0018) هذه الدراسة تمت عدديا مع الاخذ بعين الاعتبار الظواهر المرتبطة بالتدفق حول هاته الاجنحة. تم محاكاة التدفق حول توربين الرياح هذا باستخدام ANSYS18.2. تم استعمال تسلسل عملي لتصميم التوربين, ثم استخدام التصميم في المعالج لتوليد الشبكية باستخدام تقنية الانزلاق لمحاكاة دوران هذا التصميم. تم استخدام نموذج الاضطراب k- ϵ وتم وضع المحاكاة عند سرعة رياح السنوية في المنطقة 3.8 م/ث. نتائج المحاكاة استعملت كمرجع من اجل التحقق من صحة التصميم لغياب اختبار النفق.

الكلمات الدالة: توربين المحور العمودي , تقنية شبكة الانزلاق, معالجة التدفق الديناميكي, ANSYS®, التدفق المتغير, NACA0018

Résumé

Dans cette mémoire, l'écoulement instationnaire de dimension 2D autour d'une éolienne à axe vertical H-Darrieus (VAWT) comprenant trois profils aérodynamiques rotatifs (NACA0018) a été étudié numériquement en considérant le sillage proche. L'écoulement autour de l'éolienne a été simulé en utilisant ANSYS 18.2. Un flux de travail pour la conception a été utilisé pour optimiser les performances du rotor puis, un CFD a été utilisé comme pour générer la grille pour le rotor proposée un maillage de sliding mesh a été générer. Un modèle de turbulence k- ϵ a été utilisé pour l'analyse et la simulation a été réglée à la vitesse du vent de la région de 3,8 m / s. En raison de l'absence de test en tunnel les résultats de la simulation ont été utilisés comme référence afin de valider la conception.

Mots clés: H-Darrieus Eolienne, Technique de Maillage Coulissante, ANSYS®, L'écoulement instationnaire, NACA0018